FACULDADE DE ENGENHARIA DA UNIVERSIDADE DO PORTO

# Design of an autonomous system for monitoring the integrity of a structure

**Vitória Maria Ribeiro Vieira**

FEUP FACULDADE DE ENGENHARIA UNIVERSIDADE DO PORTO

Master's in Mechanical Engineering

Supervisor: Mário Augusto Pires Vaz

Second Supervisor: Nuno Viriato Ramos

July 21, 2023

# Design of an autonomous system for monitoring the integrity of a structure

**Vitória Maria Ribeiro Vieira**

Master's in Mechanical Engineering

July 21, 2023

# Abstract

The increasing demand for reliable and efficient structural health monitoring has led to the development of innovative technologies. Accurate measurement of deflection is crucial for evaluating structural safety, yet it remains a challenging task. Inclinometers have shown promise in deflection measurements for highway and railway bridges, offering high-precision results.

The objective of this work is to introduce an approach to assess the structural integrity of a longitudinal structure in flexion (i.e. bridges) through an autonomous monitoring system. Various types of inclinometers are presented, and different methods for deflection estimation are proposed based on the number of inclinometers deployed. To validate the effectiveness of the methods using either two or a single inclinometer, experimental tests were conducted on a simply supported beam. Practical considerations were also discussed.

Future studies can explore additional applications and optimization of the monitoring system. The proposed autonomous system has the potential to enhance the safety and reliability of bridges by providing real-time information on structural integrity.

**Keywords**: Structural health monitoring, deflection estimation, inclinometers

# Resumo

A procura crescente de uma monitorização fiável e eficiente do estado das estruturas levou ao desenvolvimento de tecnologias inovadoras. A medição exata da deflexão é crucial para a avaliação da segurança estrutural, mas continua a ser uma tarefa difícil. Os inclinómetros têm-se revelado promissores na medição de deflexões em pontes rodoviárias e ferroviárias, oferecendo resultados de elevada precisão.

O objetivo deste trabalho é apresentar uma abordagem para avaliar a integridade estrutural de uma estrutura longilínea em flexão (como o caso das pontes) através de um sistema de monitorização autónomo. São apresentados vários tipos de inclinómetros e propostos diferentes métodos de estimativa da deflexão com base no número de inclinómetros usados. Para validar a eficácia dos métodos que utilizam dois ou um único inclinómetro, foram realizados ensaios experimentais numa viga simplesmente apoiada. Foram também discutidas considerações práticas.

Estudos futuros podem explorar aplicações adicionais e a otimização do sistema de monitorização. O sistema autónomo proposto tem o potencial de aumentar a segurança e a fiabilidade das pontes, fornecendo informações em tempo real sobre a integridade estrutural.

**Keywords**: Monitorização da condição estrutural, estimativa da deflexão, inclinómetros

# Acknowledgements

I would like to start by thanking my supervisors professor Mário Vaz and engineer Nuno Viriato Ramos for their guidance throughout this work, giving me knowledge, material to work with and news of falling bridges.

A special thanks to the INEGI institute and the LOME section for allowing me to use the laboratory for the experiments.

A big thank you to all my friends that accompanied me during the good and trying times. The biggest acknowledgement to my parents that supported me in more than one way in all my years of existence, with love, care and encouragement, and to brother, for being much more than a sibling, for being a friend, someone to rant about academic frustrations, and for the patience with all my silliness. To my family, thank you and I love you.

An honourable mention to all my professors that passed their knowledge throughout all these years, they are masters and I was one of many pupils.

Vitória Maria Ribeiro Vieira

*"Jump and you will find out*
*how to unfold your wings as you fall"*

Ray Bradbury

# Contents

# List of Figures

# List of Tables

# Abbreviations

| | |
|---|---|
| NDT | Non-destructive Testing |
| NDE | Non-destructive Evaluation |
| SHM | Structural Health Monitoring |
| LVDTs | Linear Variable Differencial Transformers |
| NHS | National Highway System |
| IP | Infraestruturas de Portugal |
| MEMS | Microelectromechanical Systems |

# Chapter 1

# Introduction

## 1.1 Background and Motivation

Infrastructure safety and integrity has always been a fundamental concern for decision-maker authorities. Structural failure due to degradation and hazardous events has led to not only casualties but also direct and indirect economical losses, threatening societies' well-being in massive scales. To understand existing structures' behavior against natural and man-made demands, performance evaluation methods with structural analysis and local material sampling frameworks have been the main guidelines for the past few decades. However, these methods work heavily on a simulation basis, which may deviate from the actual behavior due to the large uncertainty level of infrastructure systems.

Recent progresses made in sensor and information technology offered a data-driven alternative to incorporate actual global structural behavior through vibration-based Structural Health Monitoring methodologies.

Structural Health Monitoring (SHM) has evolved over time with advancements in compact and affordable sensor technology, as well as the capacity to swiftly process and analyze large volumes of data. The current state of technology has made it both economically viable and straightforward to deploy monitoring systems. In the past, traditional approaches primarily relied on periodic human inspections and physical tests. However, industries such as aerospace and mechanical engineering were early adopters of monitoring systems. Electrical sensing systems have long been integrated into airplanes and vehicles, whereas resistance persisted when it comes to monitoring structural assets.

The unsatisfactory condition of bridge structures can be attributed to many factors, including inadequate inspection and monitoring of existing structures. Regular inspections and assessments are crucial to ensure the soundness of bridges. While visual inspection and Non-destructive Testing and Evaluation (NDT/NDE) have been traditionally employed to assess structural health, they suffer from subjectivity and periodicity limitations. Continuous monitoring emerges as the optimal solution to address these challenges.

Figure 1.1: A rescue helicopter circles above the remains of the bridge on March 5, 2001 [1]

The primary objectives of bridge monitoring encompass gathering quantitative data on structural behavior to validate design assumptions, providing real-time feedback during construction (particularly relevant for new bridges), and evaluating the current condition of bridges. This information empowers engineers to make informed decisions regarding future actions and facilitates proactive planning for maintenance and repair, particularly for existing bridges. By implementing a monitoring system, the safety of structures can be enhanced, and early warnings can be issued for any acceleration of known degradation. Furthermore, the field of SHM has witnessed an increasing application in extending the lifespan of bridges with known issues through controlled measures, contributing significantly to their safety and longevity in recent years.

This approach can be of extreme help to prevent bridges failure accidents and avoid repeating tragic events such as the Entre-os-rios bridge collapse in Portugal in 2001, which claimed 59 lives, or the Morandi bridge collapse in Genoa, Italy, in 2018, resulting in 43 deaths and 600 displaced individuals. As indicated by Euronews [1], the bridge connecting Entre-os-Rios to Castelo de Paiva in northern Portugal, Figure 1.1, was over 110 years old when it tragically collapsed. The implementation of a basic monitoring system, such as the installation of inclinometers, could have provided evidence of the bridge's inadequacy and the imminent danger of collapse.

Regarding the Morandi bridge incident, Figures 1.2 and 1.3, as reported by BBC news [2], it has been revealed that there was prior knowledge for years about the potential risk of collapse. Gianni Mion, the former head of the highways company responsible for the bridge and its maintenance, has expressed his regret for overlooking this risk. Once again, the availability of data from a monitoring system could have provided crucial confirmation to prompt necessary actions, such as closing the bridge and conducting the required maintenance or even demolition (especially considering the existing evidence of risk, such as cable corrosion). This tragedy could have been prevented through appropriate intervention.

In situations like these, a simple inclinometer system could be programmed to send a signal to


Figure 1.2: Colapse of the Morandi bridge in 2018 [2]

a gate or traffic lights installed at the entrance of the bridge. This signal would prompt the closure of the bridge for traffic in the event of any potential risk of collapse.

According to the U.S. Department of Transportation, in the Transportation Statistics Annual Report 2022, "the number of the Nation's bridges in poor condition declined from 59,305 bridges (about 10% of all bridges) in 2010 to 42,966 in 2022 (6,9%). Poor bridge conditions affect freight transportation and passenger travel, especially if detours around a closed bridge or weight restrictions are in place. Under extreme circumstances, poor bridge conditions can lead to headline grabbing catastrophic failures and collapses. The percent of bridges in poor condition has been two-and a-half to almost three times greater for non-NHS bridges than for NHS bridges." (NHS – National Highway System). In Portugal is an important subject as well. On the 16th of May 2023, the state-owned company "Infraestruturas de Portugal" released the "50 Innovation Challenges of IP" ("50 Desafios de Inovação da IP" in portuguese) in which they promote an open innovation program with 50 Innovation Challenges aimed at finding solutions for the needs of the IP Group that can be addressed through collaboration with the scientific, technological, and business community [19]. Some of these challenges involve the use of sensors and remote monitoring of several infrastructures such as railroads, tunnels and art pieces ("D16. Instrumentation of the railway infrastructure"; "D17. Remote Monitoring Systems for Infrastructures").

As seen, SHM plays a crucial role in ensuring the safety, reliability, and longevity of various infrastructure systems, including bridges, buildings, dams and pipelines. It involves the continuous monitoring and assessment of these structures to detect any damage, defects, or changes in their structural integrity.

The importance of increasing the utilization of SHM lies in its ability to enhance the overall safety and performance of infrastructure systems. Traditional inspection methods, which rely on periodic visual inspections and testing, have limitations in providing a comprehensive understanding of a structure's condition. SHM, on the other hand, offers continuous monitoring, allowing

Figure 1.3: Riccardo Morandi demonstrates a model of Morandi Bridge to the then Italian president [3]

for the detection of early warning signs of potential failures or degradation. This early detection enables timely interventions, reducing the risk of catastrophic events, such as the ones presented above, minimizing the impact on public safety, and avoiding costly repairs. Furthermore, SHM provides valuable insights into the behavior and performance of structures under varying loads, environmental conditions, and aging effects. This information aids in the validation of design assumptions, improving future designs, and ensuring that structures perform as intended throughout their lifespan. By accurately assessing the structural behavior, SHM enables engineers and decision-makers to make informed decisions regarding maintenance, repair, and retrofitting strategies, optimizing the allocation of resources, and extending the life cycle of structures.

One of the challenges that has hindered the wider adoption of SHM is the associated costs. Implementing a comprehensive SHM system can be expensive, involving the installation and maintenance of sensors, data acquisition systems, and data processing infrastructure. The upfront costs, as well as ongoing operational expenses, have been a barrier for many organizations, particularly those with limited budgets or competing priorities. Reducing the cost of SHM is of paramount importance to promote its wider adoption and maximize its benefits. Advances in sensor technologies, data processing techniques, and wireless communication have contributed to cost reduction in recent years.

By embracing SHM and promoting cost-effective solutions, we can enhance the resilience, durability, and sustainability of our infrastructure systems, ensuring their long-term viability and contributing to the overall well-being of society. One way to reduce these costs, is to carefully select the type of sensors to be used.

Knowing the deflection of a structure is crucial in various scenarios, including the monitoring of bridges. There are several methods available to determine deflection accurately. One approach involves using optical or electronic leveling devices combined with surveying techniques. This method entails measuring the change in vertical elevation at specific points on the structure. By comparing the elevations before and after applying a load, the deflection can be calculated. Differential displacement sensors, such as linear variable differential transformers (LVDTs) or displacement transducers, are commonly employed to directly measure the displacement or deflection of specific points on a structure. These sensors provide precise and accurate measurements along a single axis, allowing for accurate deflection analysis. Strain gauges are another useful tool for measuring deflection. These devices measure strain, which is the deformation or elongation of a material under load. By strategically attaching strain gauges to the structure, changes in strain can be measured and used to calculate deflection accurately. Optical methods, such as laser-based technologies or digital image correlation, offer another approach to measure deflection. These techniques utilize cameras or laser systems to track the movement of markers or patterns on the structure. By analyzing the captured data, the corresponding deflection can be determined. Load cells, which measure the applied load on a structure, can also be utilized. By applying known loads and measuring the resulting deflection, it becomes possible to establish the relationship between the load and deflection for accurate analysis. Inclinometers are sensors designed to measure the angular displacement or tilt of a structure. By strategically installing inclinometers at key locations, such as on beams or columns, the deflection or rotation of structural elements can be monitored effectively.

It's important to consider the specific requirements and constraints of the project when choosing between strain gauges and inclinometers. Both methods have their advantages and disadvantages, and the selection should be based on factors such as accuracy requirements, installation complexity, measurement type (angular vs. linear), and cost considerations.

## 1.2 Dissertation objectives and structure

### 1.2.1 Objectives

In real-life structures such as bridges, occasional overloads resulting from weather conditions or improper handling can cause damages that, if detected early, can help prevent accidents. To address these challenges, the implementation of sensors and data collection and analysis systems becomes essential for monitoring structural safety and accident prevention. In this work, the aim is to validate the effectiveness of inclinometers as sensors for data collection and prediction of structural deflection in such applications.

### 1.2.2 Structure

The following dissertation is divided into the following chapters:

Chapter 1: Introduction | In this chapter, an overview is provided on the significance of Structural Health Monitoring (SHM) in modern structures. The need for SHM to evolve is emphasized, drawing insights from past catastrophic events to prevent their recurrence.

Chapter 2: State of the Art | Chapter 2 delves deeper into SHM, discussing its methodology and the application of inclinometers as sensors. Different types of inclinometer sensors are explored based on their working principles.

Chapter 3: Deflection Prediction Methods | This chapter investigates various methods for predicting a structure's deflection based on inclination values measured with inclinometers. Examples of their implementation are presented, highlighting differences in approaches based on the number of inclinometers used.

Chapter 4: Single Inclinometer Method Testing | Chapter 4 focuses on the experimental aspect of the study. It begins by describing the preparation of the experiment and then presents the results for both measured and predicted deflection values of the tested structure. A comparative analysis of the results is conducted.

Chapter 5: Conclusion | In the final chapter, conclusions are drawn regarding the effectiveness of inclinometers in a simple monitoring system. Additionally, suggestions for further research and development are provided.

# Chapter 2

# State of the Art

Structural Health Monitoring (SHM) is an essential field of study that focuses on continuously monitoring the performance and condition of structures and systems to ensure their integrity and safety. It involves the use of various sensors, data acquisition systems, and analysis techniques to gather and interpret data related to the behavior and health of a structure. By monitoring structures over time, SHM aims to detect any signs of damage, defects, or changes that may occur, enabling timely intervention and maintenance.

SHM involves the deployment of a range of monitoring techniques to collect data on the behavior and condition of a structure. These techniques include the use of sensors that measure parameters such as strain, vibration, displacement, temperature, humidity, and corrosion. The data acquired from these sensors is then processed and analyzed using sophisticated algorithms and analytical tools to assess the health and performance of the structure.

The field of SHM has with wide-ranging applications across multiple industries. Its significance extends to civil infrastructure, aerospace, energy, transportation, and more. In the realm of civil infrastructure, where bridges and highways endure substantial loads and face environmental challenges, SHM emerges as a vital tool to combat structural degradation. By embracing SHM strategies, governing bodies and authorities can adopt a proactive approach to monitor the condition of bridges, identify early indicators of damage or deterioration, and execute timely maintenance or repair interventions. Through this proactive monitoring, SHM empowers stakeholders to safeguard the integrity and longevity of critical infrastructure assets, ensuring the safety and functionality of these essential components of our modern world.

SHM can be subdivided into four subcategories in terms of type of field testing (static or dynamic testing) and the timescale of how data is physically collected (periodic or continuous monitoring) [20].

Static testing involves assessing the response of a structure under static loads, such as gravitational forces or constant applied loads. It helps evaluate deformation, stress distribution, and load-carrying capacity. Static testing is commonly used for load testing, where predetermined loads are applied to assess performance and validate design assumptions. It is beneficial for assessing structural integrity, identifying material properties, and detecting potential weaknesses or deformations that occur over time. On the other hand, dynamic testing focuses on understanding how a structure responds to dynamic forces and vibrations. It provides insights into natural frequencies, mode shapes, damping characteristics, and dynamic behavior. Dynamic testing is used to identifying resonant frequencies, fatigue damage, or structural failure. Both static and dynamic testing complement each other in SHM, providing a holistic understanding of a structure's health, integrity, and performance. This integrated approach enhances the effectiveness of SHM in detecting anomalies, predicting failures, and guiding maintenance, repair, and retrofitting strategies.

In terms of data collection, periodic monitoring involves inspections and measurements at specific intervals or predetermined schedules. Various techniques, including visual inspections, sensor measurements, and non-destructive testing, are employed during these scheduled inspections to gather information about structural behavior. Periodic monitoring is suitable for low-risk structures or situations with budget constraints where continuous monitoring may not be necessary or feasible.

Continuous monitoring, however, involves real-time or near real-time data collection from sensors installed on the structure. These sensors continuously monitor parameters such as strain, vibration, temperature, or humidity, providing a continuous stream of information about structural health. Continuous monitoring offers several advantages, including the ability to capture transient events, detect subtle changes, and provide early warnings of potential issues. It is particularly valuable for critical or high-risk structures where constant monitoring is essential for safety, maintenance optimization, and prevention of catastrophic failures.

The choice between periodic and continuous monitoring depends on factors such as the criticality of the structure, available resources, cost considerations, and the desired level of monitoring detail. While periodic monitoring may be more cost-effective and practical for certain applications, continuous monitoring provides a higher level of situational awareness and enables proactive decision-making based on real-time data. Both approaches have their merits and can be tailored to specific monitoring needs to ensure the effective management of structural health.

## 2.1 Methodology of Structural Health Monitoring

While the specific details of each SHM system can vary, SHM involves sensor and data acquisition, data transfer and communication, data analysis and interpretation, and data management. An SHM system typically consists of six common components, as seen in Figure 2.1, being:

- Sensors and data acquisition networks;
- Communication of data;
- Data processing;
- Storage of processed data;

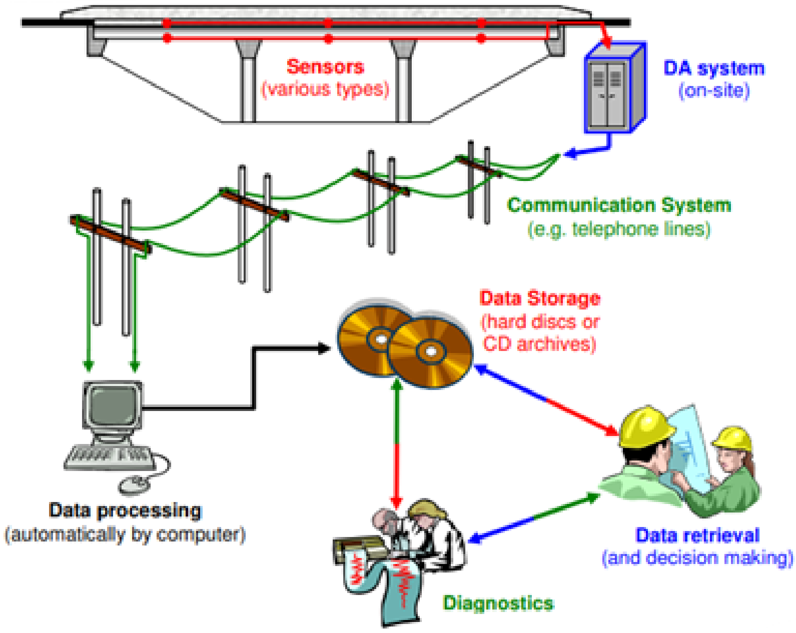


Figure 2.1: Visual schematic of a typical SHM system [4]

- Diagnostic and prognostic analysis;
- Retrieval of information as required.

### 2.1.1 Sensors

The specific types of sensors selected for a project depend on several considerations, the sensor must be able to measure the desired parameter. Another thing to consider is the conditions in which the sensor will be used, some sensors are not appropriate for long term monitoring due to deterioration in its performance. Extreme care should be taken in the selection of the number of sensors and their location within the structure. The selection criteria should also include accuracy, reliability, sensor installation limitations, power requirements, signal transmission limitations, durability, and cost [20].

Various types of sensors serve specific purposes in SHM. Strain sensors, such as strain gauges or fiber optic sensors, measure the strain or deformation experienced by a structure. In most cases, strain is measured to determine the degree of wear and thus the tension of a material through mechanical stress [21]. At the same time, measurement of the strain can also provide information about the force causing the strain.

An accelerometer is a sensor that measures the acceleration acting on an object. It can detect variation in acceleration, like gravity.

Displacement sensors, such as linear variable differential transformers (LVDTs) or displacement transducers, directly measure the linear displacement or deflection of specific points on a structure. These sensors provide precise measurements of structural deformations or movements along a single axis. Displacement sensors are used to assess the performance and behavior of structures under various loading conditions, allowing for the evaluation of structural response and deflection. They are particularly useful for monitoring the linear movement or deflection of structural elements.

Inclinometer are sensors used to measure the magnitude of the inclination angle or deformation of any structure. The inclination is either depicted in percentage or degrees concerning gravity [22]. These sensors will be explored in this chapter.

Temperature sensors monitor the temperature variations in structures. They are employed to assess the effects of temperature on material properties, thermal expansion, and potential thermal-induced stresses or deformations.

Moisture sensors detect the presence or moisture content in structures. They are used to monitor the moisture levels within concrete, soil, or other porous materials, which can cause corrosion, degradation, or structural instability.

Load cells measure the applied load on a structure, mainly the weight of objects. They are used to determine the load-carrying capacity, evaluate structural response under various loading conditions, and assess the structural safety and performance.

Acoustic wave sensors detect mechanical or acoustic waves. As the acoustic wave propagates through the material, any changes to the characteristics of the propagation path affect the velocity and/or amplitude of the wave. Changes in velocity can be monitored by measuring the frequency or phase characteristics of the sensor and can then be correlated to the corresponding physical quantity being measured [23]. They are used to identify and locate hidden damage, including delamination, corrosion, or crack propagation.

The instructions of the sensors providers need to be followed and great care should be taken during the design of the SHM system to ensure that the sensors can be easily installed without significantly changing the behavior of the structure (considering wires, conduit, junction boxes and other accessories) [20].

A detailed set of installation specifications should be prepared for each type of sensor and data acquisition component that will be used. These specifications should include the methodology and techniques used in the installation process, verification of the sensors and data acquisition components performance [20].

### 2.1.2 Data acquisition (DAQ) system and Data communication

Data acquisition (DAQ) networks are used to physically collect raw data from sensors such as strain gauges, displacement transducers, accelerometers, inclinometers, etc. The DAQ system, often called data-logger, is the onsite system where signal demodulation, conditioning and storage of measured data are conducted prior to being transferred to an offsite location for analysis. This is also the procedure where the analog output signals from sensors are converted into engineering terms, therefore all sensors must communicate with the DAQ system by either wired or wireless connection [20].

Most sensor manufacturers offer data loggers (wired or wireless) with their sensor products. There are also manufacturers who only provide data loggers which are compatible with most commercially available sensors [20].

SHM data can easily become exceptionally large in quantity especially when the structure is extensively instrumented with a variety of sensors in a variety of locations, particularly in the case of continuous monitoring [24]. A well-designed data acquisition algorithm-data sampling and recording, which captures an adequate amount of data, is a vital component of a successful SHM system and will affect both the volume of stored data and the type of diagnostic information that can be obtained [20].

In setting up the data sampling rate, the amount of data should be enough to not jeopardize its usefulness but not too much since it can overwhelm the interpretation. In some cases, as in the case of dynamic testing, high sampling rates are required to accurately measure the structure's response to transient loads. It is important to sample data at the appropriate rate for the type of testing which is being conducted. Decisions regarding appropriate sampling rates should be based on experience [20].

Data communication is a mechanism that transfers data from the DAQ system to the location where it will be processed and analyzed. The data communication mechanism allows monitoring to occur remotely and eliminates the need for site inspections. SHM systems transmit field data remotely through telephone lines, the internet or using wireless technology like radio or cellular transmission [20].

### 2.1.3 Data Processing and Analysis

Due to the many possible sources of error and uncertainty in the field, the data obtained by the various sensors in a structure are likely to contain irrelevant information and noise. One method for data quality assurance is to implement quality control at multiple levels of the signal path. At the level of the sensors and data acquisition hardware, a thorough initial calibration of the sensors and data acquisition hardware followed by periodic re-calibration of these components, verifying and ensuring the quality of the initial installations. Elementary data checks can also be programmed in the data acquisition software to automatically validate and process the data before it can be stored for later interpretation and analysis. The goal of intelligent processing is to remove this unwanted or redundant information. The various data management strategies should be able to eliminate unnecessary data without sacrificing the integrity of the overall system [20].

Selection of the most appropriate data acquisition algorithm is a critical component of SHM as it will affect both the volume of stored data and the type of diagnostic information that can be obtained. An algorithm is a set of rules or computational procedure for solving a problem [20].

### 2.1.4 Storage of processed data

The processed data can then be stored for later use in structural health diagnostics. In some cases, the data could be stored for extended periods of time, and it is important that, once retrieved, the data are easy to understand. The medium for storage of the data should allow the data to be available for an extended period (many years) without susceptibility to corruption. The amount of memory required for storage can be large in SHM applications with numerous sensors or higher data sampling rates, and care must be taken to ensure that sufficient memory is available to store all the data which will be generated. It is also important to ensure that the data files contain enough information so anyone can interpret them. It is possible that the data collected could be used years in the future, so the data files should be logical and well-documented. Developing appropriate algorithms for data quality assurance, processing and archival represents the major information technology related challenges in a SHM system. It is common to disregard raw data and store only processed or analyzed data, thereby decreasing the amount of space necessary for storage. Unfortunately, discarding the raw data does not allow for reinterpretation later [20].

### 2.1.5 Diagnostics and Prognostics

Diagnostic and prognostic is the most difficult step and an important component of an effective SHM system. Diagnostics involves further interpretation of the collected and processed data, analysis of the responses of the structure, and identifying if any of the expected damage or deterioration has occurred. Diagnostics is concerned with converting the data from monitoring to useful information about the response and health of the structure [20].

The level of complexity of the analysis will change based on the needs of the monitoring program and the SHM system components. In a simple application, it may be sufficient to convert strain readings into stresses for assessment against critical limits such as yielding. Whatever the level of sophistication of diagnostic activity, an appropriate numerical model of the structure calibrated against baseline field measurements is normally required. In a long-term structural health monitoring application, the system should be able to interpret the measurement data, compare the result with some predetermined set of criteria, and execute a decision in an automated manner. The simplest example is to program a health monitoring system to issue an alert when the measurement data indicates that some behavior has exceeded a particular threshold value [20].

## 2.2 Inclinometers

Evaluating the deflection of a bridge span when subjected to designed loads is of great importance for ensuring bridge safety. However, directly measuring bridge deflections can be a challenging task, particularly for bridges located over rivers, railways, or highways. In such scenarios, the inclinometer method emerges as a promising solution. This method provides a straightforward, practical, and cost-effective approach to measure both static and dynamic deflections of bridge spans under loads, even for bridges with significant heights. Inclinometers serve as an ideal solution due to their ease of installation and the fact that they do not require an external reference. Instead, they utilize gravity, the downward acceleration, as their internal reference point, simplifying the measurement process.

Hundreds of experiments and practical tests on simple and continuous bridges, utilizing dynamic and static loads, under various vehicle speeds, show that the method has very high precision, which provides an authentic basis for new-built bridge acceptance and old bridge safety evaluation. The method does not need fixed observation positions as other deflection measurement methods because the inclinometers are installed on the bridge directly, which increases measurement efficiency greatly [18].

Inclinometers, also called tilt sensor, clinometers, or slope sensors, are designed to measure an object's angle with respect to gravity force. They determine the pitch and/or roll angle and output these values via the appropriate electrical interface [25].

Every inclinometric system requires equipment and sensors to measure and collect data. According to function and principles, the classification of tilt sensors is also different [26].

Inclinometers can be mechanical or electronic. The electronic inclinometric equipment consists of:

- The measuring sensor and all the electronic components necessary for it to work;
- The instruments body;
- The connection cable;
- the supply, acquisition, control, and storage unit(s).

Sensors can be classified as uniaxial, biaxial or triaxial, depending on how many axis they can measure the inclination, they can also be classified by the technology used (i.e. operating principle), the latter is the approach of this current work.

The reference plane of an inclinometer in the one where the inclination is zero. There are three possible types of inclinometers based on the reference plain.

- Horizontal: This refers to the level or horizontal position of an object. Inclinometers can measure the inclination of an object relative to this plane, indicating whether it is tilted to the left or right.
- Vertical: This plane represents the perpendicular orientation to the horizontal plane. Inclinometers can measure the inclination of an object relative to this plane, indicating whether it is tilted forwards or backwards.
- Arbitrary Plane: In some cases, inclinometers can be used to measure the inclination of an object with respect to a specific arbitrary plane. This could be a custom-defined reference plane that is relevant to a particular application or measurement requirement.

The latter ones are not very popular, they still exist in the marked, however some horizontal or vertical inclinometers have amplitudes that can go up to ±90°.


Figure 2.2: 5789/1 – Bubble Inclinometer [5]

### 2.2.1 Mechanical inclinometers

There are mainly two different types of mechanical inclinometers. Bubble inclinometers, Figures 2.2, also known as spirit level or bubble level, use a liquid-filled glass vial with an air pocket inside. The position of the bubble in the vial indicates the angle of inclination.

Pendulum Inclinometers, Figure 2.3, use a pendulum mechanism to measure the tilt. The pendulum is suspended within the device and its displacement indicates the inclination angle. There are also inclinometers that use a spherical small mass that moves in a scale according to the inclinometer's position, Figure 2.4. All of these rely on gravity and there is no need for recalibration.

### 2.2.2 Digital inclinometers

#### 2.2.2.1 Sensors based on Wheatstone bridge

A Wheatstone bridge, Figure 2.5, is a divided bridge circuit used for the measurement of static or dynamic electrical resistance. The output voltage of the Wheatstone bridge circuit is expressed in millivolts output per volt input. The Wheatstone circuit is also well suited for temperature compensation [27].

The resistive elements that vary along with the quantity to be observed are called active elements [28].

The circuit has four "arms" formed by resistances, R1, R2, R3, and R4. A voltage is applied between A and B and the resistance R4 is altered until no current flows between C and D. At this point, the needle of the galvanometer is not deflected, and the bridge is balanced. Since R1, R2, and R4 are known, R3 can be calculated.

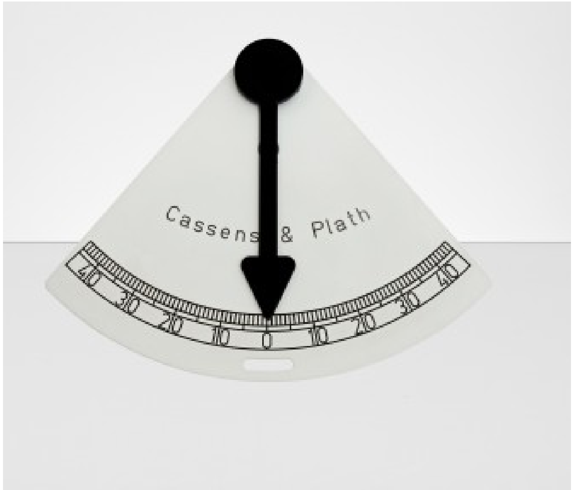


Figure 2.3: Pendulum clinometer triangular [6]

$$\frac{R_1}{R_2} = \frac{R_3}{R_4} \tag{2.1}$$

The most common Wheatstone bridge configurations are the quarter bridge networks, Figure 2.6, the half bridge networks, Figure 2.7, and the full bridge networks, Figure 2.8 [28].

Due to its convenience and fast reading speed, the unbalanced bridge is the most used. The main constraint of this technique is the variation in resistance due to thermal changes. Thermal sensitivity affects both the sensor elements and the connection cables to the reading unit, with this influence increasing with the length of the wiring. In inclinometric instruments used to profile boreholes with depths of several meters, there is a significant influence on the quality of the obtained data. To minimize the thermal effect on the wiring, the resistances used in the bridge are much higher than the resistance of the connection cables, and the bridge is configured in a way that distributes the thermal influence across multiple elements. The bridge can also be configured to increase the response signal by placing multiple elements subjected to deformation [28].

In the case of the conventional inclinometric instruments, the half bridge with two active elements (parallel or at 90° angle of each other) is the most used configuration. In this configuration, the cable resistance variation is negligible and the thermal influence on the active elements is minimized.

This methodology can be applied in three types of sensors:

- Potentiometers: half bridge with two parallel active elements.
- Pendulous: Rigid pendulum with two parallel active elements (Wheatstone half bridge), one on each side of the suspension rod. When the instrument is perturbed (inclined) the weight of the pendulum induces a deformation, tensioning the resistive elements.
- Electrolytic level: sealed glass vial partly filled with a conductive liquid. Output resistance can be read with a portable strain indicator, in which case the two resistances form two


Figure 2.4: 2110-D Mechanical Inclinometer (Rieker inc) [7]

arms of a Wheatstone bridge circuit, or the device can be read in the same way as a linear potentiometer.

Electrolytic sensors The electrolytic sensors are preferred for the fixed systems due to its low cost of acquisition and maintenance as well as low energy consumption [28].

An electrolytic level, Figure 2.9, consists of a sealed glass vial partially filled with a conductive liquid. Output resistance can be read with a portable strain indicator, in which case the two resistances form two arms of a Wheatstone bridge circuit, or the device can be read in the same way as a linear potentiometer [8].

#### 2.2.2.2 Vibrating wire sensors

Vibrating wire sensors consist of a rigid pendular system coupled to a wire of steel, tensioned between 9 – 13% of the yield stress, with an electromagnetic coil close to its midpoint. Analogously to the pendular system based on a Wheatstone bridge, there can be a configuration of two wires and two coils, one on each side of the pendulum, for a uniaxial sensor, and another with four strings and four coils for a biaxial sensor. However, there are different configurations [8,28].

There are two fundamental versions of this system:

- Open circuit (pluck and read): the coil excites the wire with an electromagnetic impulse, making it vibrate at its natural frequency, and then transmits the alternating current induced by the vibration to a frequency counter. When the pendulum is accelerated, due to the variation of the instrument's inclination, the tension in the string changes and, consequently, the frequencies of vibration and induced current increase or decrease according to voltage variation, either positive or negative, respectively. This method is used in static measurements [28].

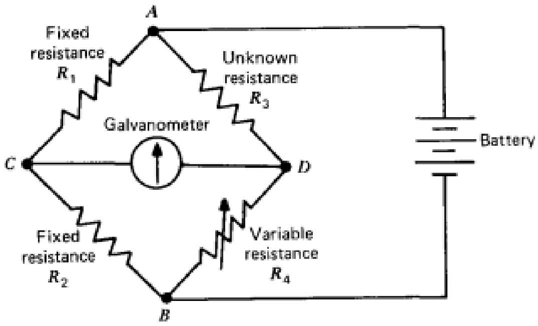


Figure 2.5: Wheatstone bridge circuit [8]

- Closed circuit (continuous excitation or auto resonant): similar to the open circuit, but a second coil is used to detect the frequency. The signal is fed back to the driving coil so that it applies a continuously pulsing voltage with frequency identical to the natural frequency of the vibrating wire. As the wire frequency changes, so does the driving frequency. This method is used for low-frequency dynamic measurements [8,28].

With this type of sensors, the response can be obtained with frequency of vibration or voltage signal. The first one is preferable since the frequency response turns negligible the effects of the resistance of the contacts and cabling have on Wheatstone bridge-based sensors, enabling longer lengths of cable. Also, the frequency is a more stable signal when compared to voltage signal [28].

The equation for frequency of a vibrating wire in terms of wire stress is:

$$f = \frac{1}{2L}\sqrt{\frac{\sigma g}{\rho}} \tag{2.2}$$

[28]

where:

$f$ = natural frequency $\left(\mathrm{s}^{-1}\right)$

$L$ = length of vibrating wire $(\mathrm{m})$

$\sigma$ = stress in the wire $(\mathrm{Pa})$

$\rho$ = density of the wire material $\left(\mathrm{kg/m}^3\right)$

$g$ = acceleration due to gravity $\left(\mathrm{m/s}^2\right)$

In terms of wire strain,

$$f = \frac{1}{2L}\sqrt{\frac{Eg\varepsilon}{\rho}} \tag{2.3}$$

Where:

$E$ = modulus of elasticity of the wire $(\mathrm{Pa})$

$\varepsilon$ = strain in the wire

The major disadvantages of vibrating wire transducers are wire corrosion, creep of the vibrating wire under permanent tension, and slippage at the wire clamping points, all of which usually

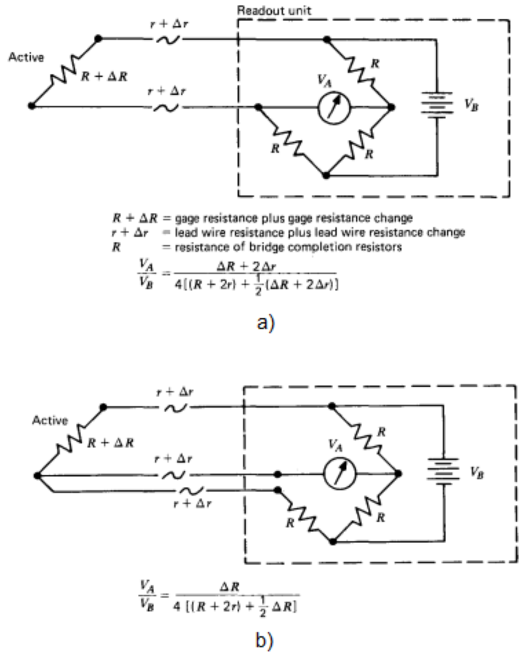


Figure 2.6: Wheatstone bridge quarter bridge networks: (a) two-wire system and (b) three-wire system (thermal compensation) [8]

result in a reduction in vibrating frequency. Corrosion can be minimized by selection of materials that are not subject to galvanic corrosion and by drying and hermetically sealing the cavity around the wire. If the vibrating wire creeps under permanent tension, or if slippage occurs at the wire clamping points, a frequency reduction occurs that is unrelated to strain, and a zero drift has occurred [8].

Like the Wheatstone bridge-based sensors, the vibrating string is sensitive to temperature changes, so the data processing involves two steps, calculation of the inclinometric variation and subsequent thermal correction. The thermal effect on the sensor response affects the linearity, so the respective correction is done by polynomial regression obtained by calibration [28].

#### 2.2.2.3 Force-balance (servo) sensors

This type of sensor, Figure 2.10, is typically more expensive compared to other types of inclinometers due to their advanced control systems, despite that it is the most widely used sensor in portable inclinometer probes since the 1980's. The advantages of these sensors that are attributed with its popularity are:

- High sensitivity;
- High resolution;
- Good linearity;

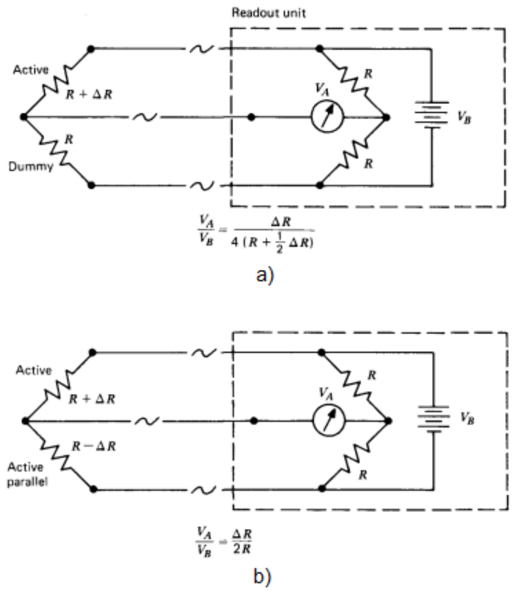


Figure 2.7: Wheatstone bridge half bridge networks: (a) dummy gauge (one active element), (b) both gauges fully active (two active elements) [8]

- Low hysteresis;
- Relative insensitivity to thermal variations after the heating period (done for prevention) [28].

The basic sequence of operation, common to all classic force-balanced servo accelerometers, can be summarized by the following sequence of events [9]:

1. The oscillator transmits an excitation signal to the sensing coils and the phase shifter.
2. The sensing coils produce a magnetic field, which varies according to the position of the eccentric mass and return a signal to the quadrature detector.
3. The quadrature detector receives signals from the phase shifter and the sensing coils and sends a signal proportional to the phase difference between the two received signals to the operational amplifier.
4. The quadrature detector receives signals from the phase shifter and the sensing coils and sends a signal proportional to the phase difference between the two received signals to the operational amplifier.
5. Based on the received signal, the drive coil moves the eccentric mass to the point where the response of the sensor coils is "in phase" with the phase shifter signal, and the output circuit generates a response signal.

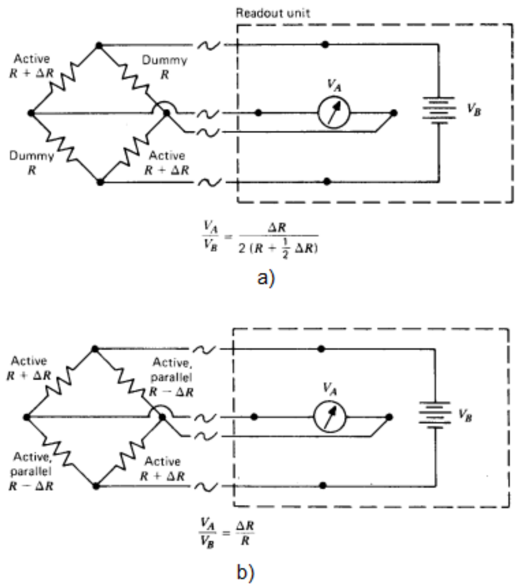


Figure 2.8: Wheatstone bridge full bridge networks: (a) dummy gauges (two active elements), (b) all gauges fully active (four active elements) [8]

The signal generated in step 4 is proportional to the displacement of the pendulum mass, and the response obtained in step 5 is proportional to the current required to generate a magnetic field that restores the mass to its equilibrium point. In fact, the measurement is performed analogously to a balanced Wheatstone bridge, but it is based on the variation of the magnetic field induced by the movement of the mass rather than the variation of resistance in a deformable element [28].

One of the main weaknesses of these sensors is shock resistance. To prevent this, the instrument must be handled with care and following all the instructions of the fabricant.

#### 2.2.2.4 Micro-electromechanical systems (MEMS)

Micro-electromechanical systems (MEMS) represent the concept of integrated production of complete systems, encompassing, in the case of metrological instruments, the sensor and the entire electronic structure of excitation, signal processing, and response.

This technology was conceptualized during the 1950s and 1960s based on the enhanced piezoresistive effect in semiconductor crystals. Although the first piezoresistive sensors for load, strain, and pressure in crystalline form emerged in the 1960s, the MEMS industry only took shape in the 1980s and established itself definitively in the late 1990s. Currently, these systems are present in virtually all electronic devices used in everyday life, medical, industrial, military, or scientific applications [28]. The wide range of applications for these sensors serves as a significant driving force for their ongoing development and technological advancement. As a result, it is anticipated that MEMS with various operating principles will be increasingly adopted in the future.

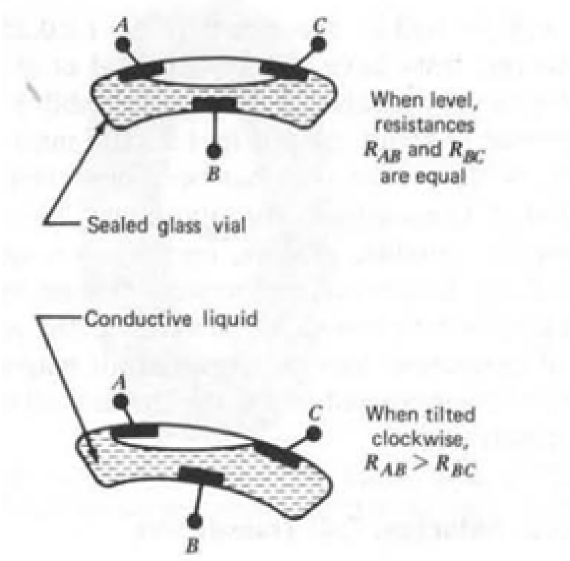


Figure 2.9: Schematic of electrolytic level [8]

MEMS inclinometers, example in Figures 2.11 and 2.12, also known as MEMS tilt sensors, are compact and highly precise devices, these sensors offer numerous advantages, including small size, low power consumption, high sensitivity, and cost-effectiveness.

By applying proper material selection, it makes possible to influence on the MEMS device processing costs, being silicon the most important staring material used in MEMS, according to Tilli et al [29].

The effectiveness of a targeted application relies heavily on choosing the right actuator. Furthermore, the overall efficiency of the actuator is influenced by various factors including power and control methods, compatibility, packaging requirements, and cost-effectiveness. MEMS devices involve a broad scope of domains to measure information from the surrounding environment and convert it to useful electrical signals. There are six domains of interests:

- Electrical domain – involve electric field, current, voltage, resistance, charge, capacitance, inductance, dielectric constant, polarization and frequency;
- Chemical domain – include composition, reaction rate, concentration, pH and oxidation or reduction potential;
- Mechanical domain – involve length, width, area, all-time derivatives such as velocity, acceleration, mass flow, volume, force, pressure, torque, acoustic wavelength and acoustic intensity;
- Thermal domain – include temperature, flow, heat, specific heat, entropy and state of any matter;
- Radiative domain – involve intensity, phase, polarization, wavelength, reflectance, transmittance and refractive index;

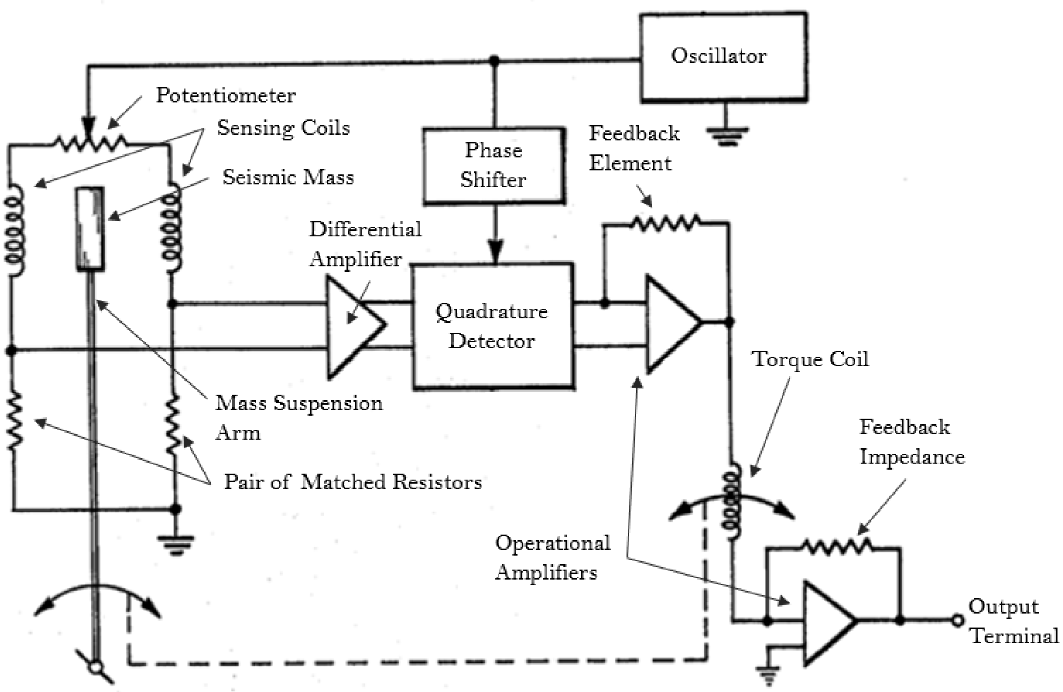


Figure 2.10: Partially schematic and partially block diagram of a force balance servo accelerometer (invented by E. Hernandez and F. Gichard) [9]

- Magnetic domain – include field intensity, permeability, flux density and magnetic moment) [23].

Piezoelectric MEMS accelerometers

Piezoelectricity refers to the phenomenon exhibited by certain materials when subjected to mechanical stress, generating an electric potential through polarization. This reversible property has been utilized since the 19th century, primarily in the form of sensors (e.g., pressure transducers) and actuators (e.g., valves), with crystals like quartz being common examples. While the application of piezoelectricity in the MEMS field is relatively recent, it requires the incorporation of piezoelectric materials into the silicon structure using methods such as thin film deposition or atomic contamination (doping) of the silicon crystal structure.

In the case of piezoelectric accelerometers, Figure 2.13, they typically rely on the deflection of a piezoelectric silicon beam. The resulting electric potential, induced by the stress exerted on the beam, is captured using a capacitance capacitor. Despite attractive features such as ease of monolithic production and intrinsic self-verification, this type of sensor experiences reduced sensitivity as it is miniaturized, and its response necessitates thermal correction. Also, the incorporation of piezoelectric elements into the crystal structure involves costly and challenging manufacturing processes. As a result, capacitive MEMS accelerometers are preferred for measuring constant acceleration, while piezoelectric MEMS, find broader application in force and pressure measurement

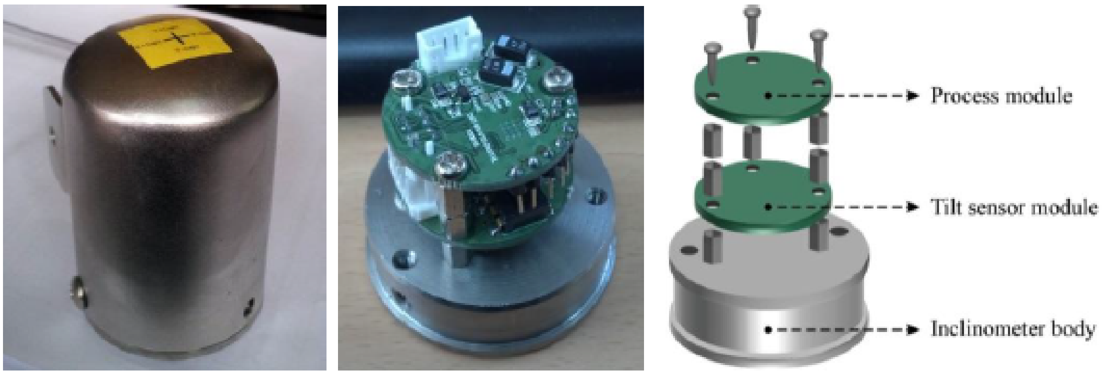


Figure 2.11: Example of a MEMS based inclinometer [10]

[28].

Piezoresistive MEMS accelerometers

This type of sensor consists of a suspended silicon platform (like a beam or rigid pendulum) connected by support elements. These support elements form the resistances of either a full or half Wheatstone bridge, like the pendulum sensors mentioned before.

Electrical conduction in semiconductor crystals, typically composed of silicon, germanium, or gallium, occurs through atomic impurities within the crystal structure. When the crystal is relatively pure, electrical conduction is well-defined. The piezoresistive effect can be amplified or reduced and is induced by the anisotropy resulting from the crystallographic configuration. By carefully controlling the level, type, and distribution of impurities within the crystal mesh (such as phosphorus, boron, arsenic, aluminum, antimony, tantalum, tellurium, among others), as well as the specific crystallographic planes utilized for electrical conduction and voltage application, the piezoresistive effect of these materials can be tens or hundreds of times greater than that of metals. Consequently, a crystalline sensor exhibits significantly higher sensitivity compared to conventional metallic sensors, enabling the detection of much smaller variations in the observed quantity.

In the 1990s these sensors were replaced by capacitive ones due to their high sensitivity to thermal variations, tendency for notable deviations and drifts, large size of the sensors, more complex and costly monolithic production and absence of inherent self-verification, necessitating an independent excitation system to ensure proper sensor functionality [28].

Capacitive MEMS accelerometers

This sensor type relies on the capacitive effect (ability to accumulate electrical charge through polarization of a non-conductive material between electrodes subjected to a differential voltage) between two closely spaced conductive elements separated by a non-conductive material. It consists of two structures, one fixed and one movable, representing the electrodes. The movable structure, supported by elastic elements, acts as the seismic mass that responds to inertial forces. As the mass accelerates and moves, the spacing between the electrodes changes, either decreasing or increasing, depending on the direction of motion. This change in spacing leads to a proportional

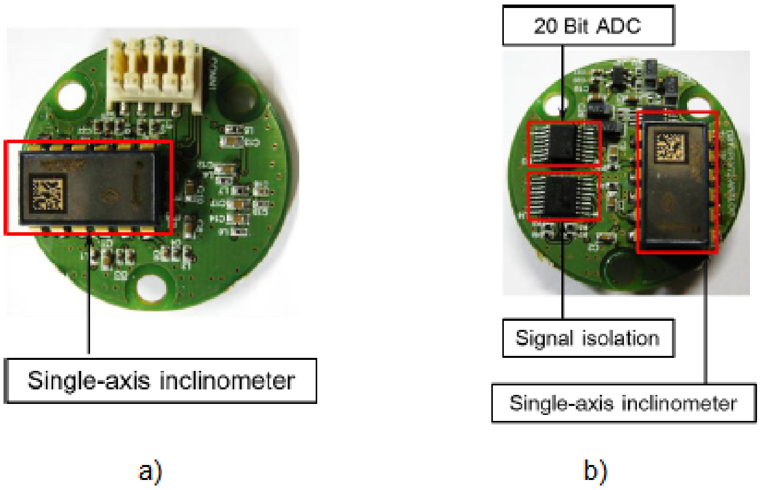


Figure 2.12: Tilt sensor module (a) upper surface, (b) lower surface [10]

increase or decrease in capacitance, reflecting the applied acceleration. The use of a differential configuration is common to enhance linearity, sensitivity, and reduce sensor errors. In precision inclinometric applications, these sensors are often servo-accelerated, operating as force-balanced servo-accelerometers, where the sensor's response is determined by the force needed to restore the mass to its equilibrium position. Notably, the variable quantity in this case is capacitance rather than magnetic induction [28].

In Figure 2.14 is represented a schematic of a uniaxial MEMS differential capacitive accelerometer, in Figure 2.15 is represented a 3D model of the same accelerometer.

These sensors have the advantages of having a better accuracy, improved linearity, thermal stability, easier calibration, less complex and cheaper monolithic production and they are intrinsically self-verifiable when servo accelerated. In contrast to classical servo-accelerometers, these sensors demonstrate greater shock resistance, lower cost, and reduced energy consumption. The only drawback mentioned is a slightly lower sensitivity for a specific measurement amplitude [28].

Thermoresistive MEMS accelerometers

The initial versions of thermoresistive MEMS accelerometers consisted of a fixed silicon base with a movable seismic mass, featuring one part heated and another equipped with a temperature measurement device. The heat diffusion between these parts, influenced by their spacing, allowed for the deduction of the gravitational acceleration acting on the sensor.

The more recent iterations, characterized by advancements in technology, do not incorporate moving parts. Instead, they are based on convective heat transfer of a heated gas bubble, Figure 2.16. These contemporary designs exhibit a simple and monolithic structure that can be produced using a single manufacturing process. The accelerometer comprises a silicon base with a cavity, where a central heating element is suspended. Additionally, a series of other temperature measurement elements are arranged diametrically and parallelly to the central element. By applying

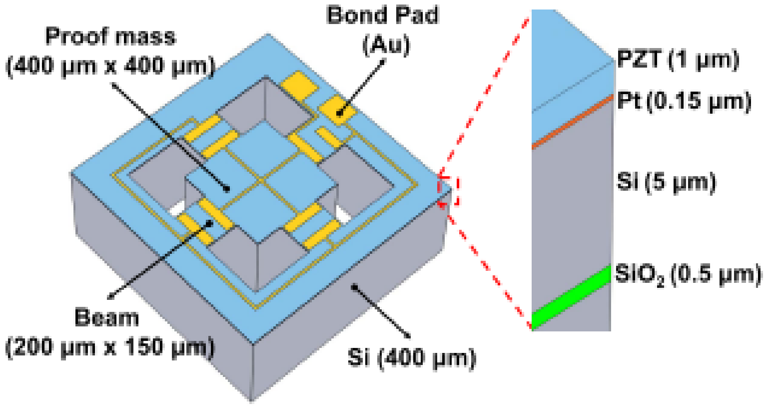


Figure 2.13: Schematic of a uniaxial piezoelectric device consisting of a proof mass with four support beams [11]

heat to the central element, a small heated gas bubble is formed, which moves along the cavity in response to the applied acceleration. The thermal distribution profile along the cavity enables the determination of the acceleration value.

The temperature measurement circuit utilizes a Wheatstone bridge configuration, employing sensory elements such as thermistors (resistors whose resistance varies with temperature, exhibiting a Negative Temperature Coefficient where resistance increases as temperature decreases, or a Positive Temperature Coefficient where the opposite occurs) or coupled thermocouples. The utilization of thermocouples allows for notable energy consumption reduction and enhanced sensitivity. Sensitivity is directly influenced by energy consumption, such as the temperature at which heating occurs, and can also be improved by increasing gas density, substituting the gas with a viscous fluid, or optimizing the sensor's geometry.

Thermoresistive MEMS accelerometers offer several advantages including enhanced shock resistance (these accelerometers do not have any moving parts or flexible supports, making them highly resistant to shock), reduced susceptibility to drift, good linearity, insensitivity to electromagnetic influences and very low cost as they incorporate simple and robust structures that are easy and quick to produce, requiring a single manufacturing process. However, they have some disadvantages as well like high energy consumption, reduced sensitivity that is dependent on ambient temperature, requiring effective thermal insulation, limited sensitivity and they have a long response time when compared to other accelerometers [28].

Electrolytic MEMS accelerometers

There are two types of electrolytic MEMS, the electroresistive, that work just like the electrolytic sensors, and the capacitive type.

The second type of sensors operates by measuring the capacitance between two electrodes that are partially immersed in a dielectric solution (liquid that insulates and separates electrical components). The capacitance value changes proportionally with the portion of the electrode that is submerged.

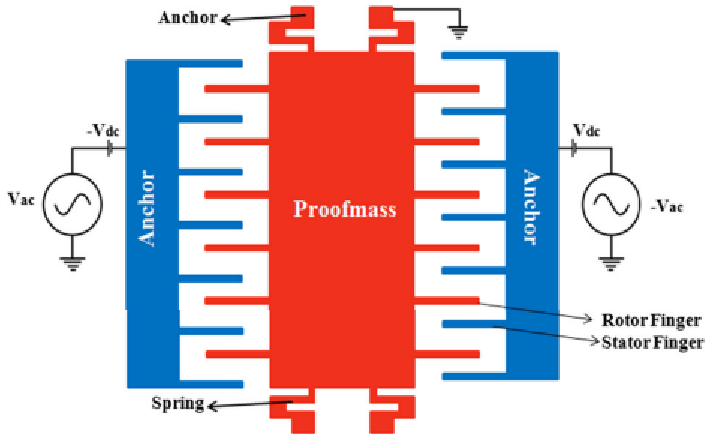


Figure 2.14: Schematic of a uniaxial MEMS differential capacitive accelerometer [12]

Electrolytic MEMS accelerometers offer several advantages, including high sensitivity, wide frequency range, and low noise levels. They are also suitable for measuring both constant andvariable accelerations. However, they have some limitations, they require a stable and controlled environment due to their sensitivity to temperature and humidity variations. They may also have higher power consumption compared to other types of MEMS accelerometers. Additionally, electrolytic solutions used in these sensors may introduce potential reliability issues, such as evaporation or contamination.

Optical MEMS accelerometers

Optical MEMS accelerometers, Figure 2.17, work by utilizing light interference or other optical phenomena. They consist of a small movable structure, like a proof mass, suspended inside the device. Light travels through a fiber optic cable within the accelerometer. When acceleration is applied, the proof mass moves, changing the space in the light path and altering the light transmission. This change in transmission affects the light intensity, which is then detected by a photodetector. The proof mass includes a finger that blocks half of the light path when there is no external acceleration. By analyzing the optical signals, the accelerometer can determine both the magnitude and direction of the applied acceleration [14].

Advantages of optical MEMS accelerometers include high accuracy and precision in measuring acceleration, as optical sensing technology can provide extremely sensitive and reliable measurements. They also offer excellent stability over time and resistance to environmental factors such as temperature variations or electromagnetic interference. Optical MEMS accelerometers are often compact and lightweight, making them suitable for applications where size and weight constraints are important.

Nevertheless, optical MEMS accelerometers also have some limitations. They can be more complex and costly to manufacture compared to other types of MEMS accelerometers. The optical components and sensors used in these accelerometers may be sensitive to alignment and

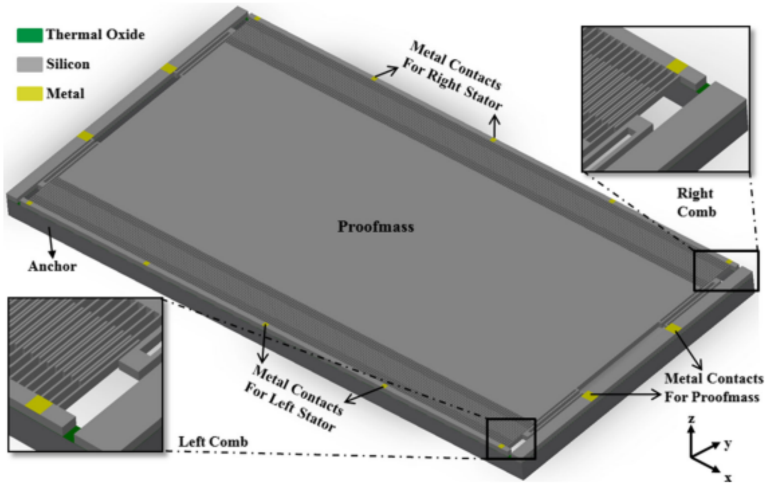


Figure 2.15: 3D solid model of a uniaxial capacitive MEMS accelerometer [12]

require careful assembly. Furthermore, optical MEMS accelerometers typically require external light sources and complex signal processing techniques, which can add complexity to the overall system. Despite these challenges, the high performance and precision of optical MEMS accelerometers make them well-suited for various applications in industries such as aerospace, automotive, and robotics.

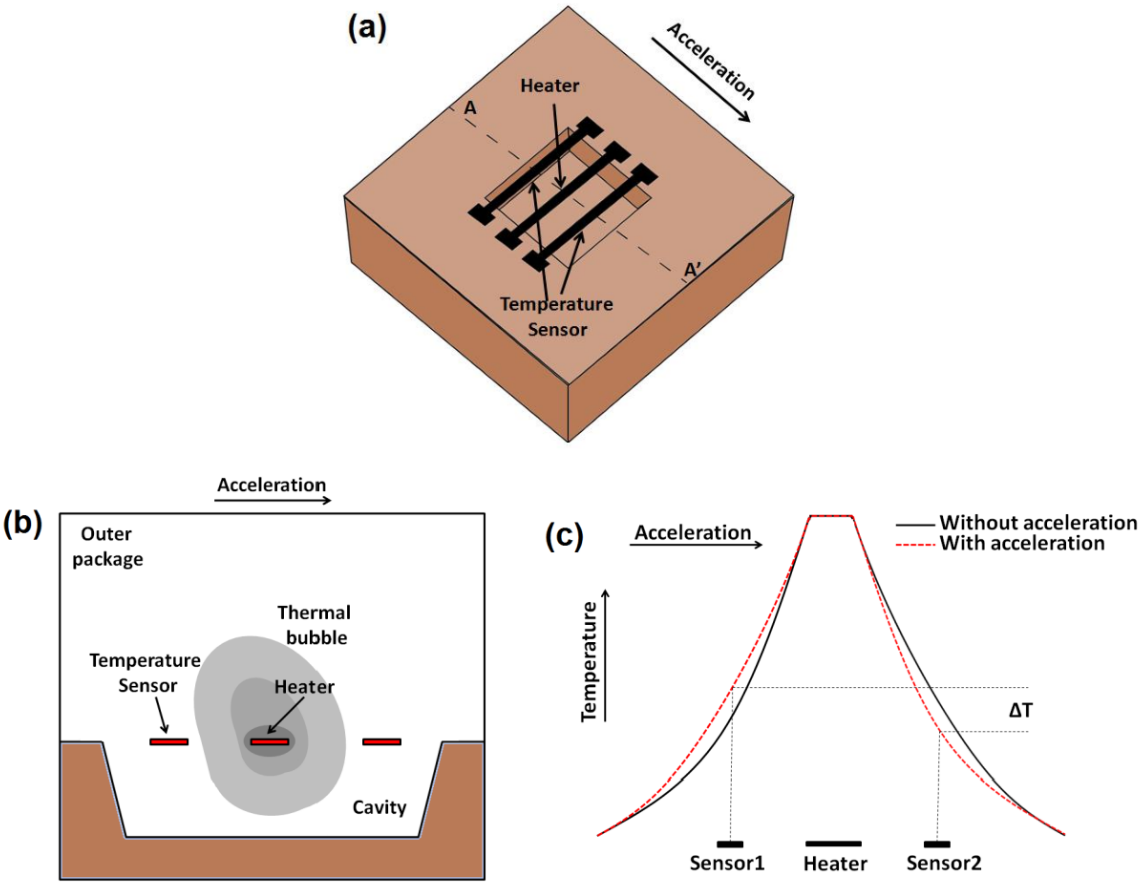


Figure 2.16: (a) schematic view of thermal accelerometer, (b) cross sectional view along $AA'$ line, and (c) temperature profile along $AA'$ [13]

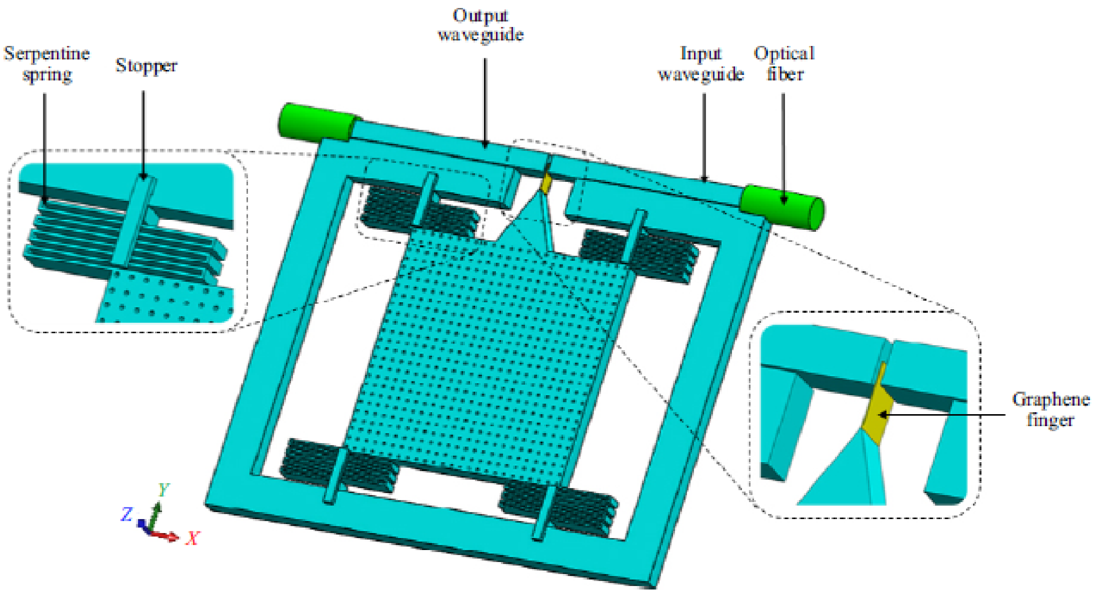


Figure 2.17: Example of an optical MEMS accelerometer structure with a graphene finger [14]

# Chapter 3

# Deflection Prediction Methods

Measuring the deflection of a bridge span under designed loads is critical to evaluate bridge safety. However, directly obtaining bridge deflections is often challenging, especially for bridges over rivers, railways, or highways. In this context, using inclinometers presents a promising solution. This method offers a simple, practical, and cost-effective way of measuring static and dynamic deflections of bridge spans under loads, even for bridges that traverse great heights.

Inclinometers can vary in price and technical specifications. For systems that do not require high measurement resolution, mechanical inclinometers such as the one from Gate14 (Figure 3.1) can be used, offering a resolution of ±0,5 degrees and costing approximately 19€. For improved resolution, a digital inclinometer like the one from Neoteck (Figure 3.2) is available, providing a resolution of ±0,05 degrees at a cost of around 24€. If the system demands extremely high resolution with minimal inclination variations, an electrolytic tilt sensor like the one from Fredericks Company (Figure 3.3) is recommended, offering a remarkable resolution of ±0,0003 degrees at a cost of approximately 40€.

As mentioned earlier, implementing a straightforward monitoring system that predicts deflection based on inclination values can be beneficial.

Extensive experiments and practical tests conducted on simple and continuous bridges, involving dynamic and static loads at different vehicle speeds, have consistently demonstrated the method's exceptional precision. This establishes a reliable foundation for assessing the safety of existing bridges and validating the acceptance of newly constructed ones. Unlike other deflection measurement methods, this approach does not require fixed observation positions, as the inclinometers are directly installed on the bridge. As a result, measurement efficiency is significantly enhanced [18].

As stated by Riqing LAN, Yushi WANG, and Qinglei CHI, there are several advantages to using inclinometers [18]. Firstly, the method is only slightly influenced by environmental conditions when the instruments are placed directly on the deck. Secondly, deflection measurements

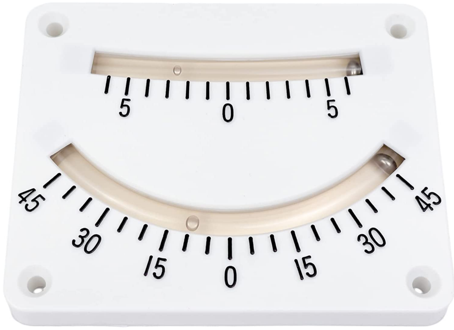


Figure 3.1: GATE14 Precision Dual-Bubble Nautical Inclinometer [15]

obtained from inclinometers do not include the subsidence of piers and deformation of bearing supports [18].

Overall, the inclinometer method offers significant engineering application value and a promising future as a potential method of measuring bridge deflection. Its simplicity, practicality, and cost-effectiveness make it an ideal solution for monitoring and evaluating bridges safety.

## 3.1 Five or more inclinometers

According to Xingmin Hou et al [18], to calculate the deflection of a bridge span based on the angular records, first it is assumed that n inclinometers are installed along a line paralleling the span axis. One can obtain n angular values for static measurement or angle time histories for dynamic measurement.

The following equations will refer to dynamic deflection, static deflection can be obtained by omitting the parameter t (time).

Defining the total measuring time as $T$, and the length of the bridge span as $L$. Angular time histories $\theta_i(t)(i = 1,2,\ldots,n; 0 \leq t \leq T)$ at $n$ controlling positions can be acquired based on the voltage outputs of $n$ inclinometers. The deflection time history $y(x,t)(0 \leq x \leq L; 0 \leq t \leq T)$at $x$ will be known if $y(x,t_0)$ at any time $t_0\,(0 \leq t_0 \leq T)$ is calculated [18].

Defining the $n$ angular values of the span at $t_0$ as $\theta_i(t_0)\,(i = 1,2,\ldots,n)$ properly selecting the deflection curve $y(x,t_0)$ of the span as

$$y(x,t_0) = A(x) \sum_{j=1}^{n-1} X_j(t_0)\, g_j(x) \tag{3.1}$$

where $g_j(x)$ is an appropriately selected function group (simplest function group in j − 1 order power series) and $X_j(t_0)$ is an undetermined coefficient, which only depends on time $t_0$ . $A(x)$ is a chosen function such as to make the deflection curve satisfy boundary conditions at the piers [18].

According to the n angular values at $t_0$ , one can obtain [18]


Figure 3.2: Neoteck Backlight LCD Digital Angle Finder [16]

$$\left[ A'(x) \sum_{j=1}^{n-1} X_j(t_0) g_j(x) + A(x) \sum_{j=1}^{n-1} X_j(t_0) g'_j(x) \right]_{x=x_i} = \theta_i(x, t_0) \quad (i = 1, 2, \ldots, n) \tag{3.2}$$

where $x_i$ is the coordinate of the $i^{th}$ inclinometer and $A'(x)$ and $g'_j(x)$ are the first differentiation of functions $A(x)$ and $g_j(x)$. The least-square method is a convenient approach to solve for the unknown coefficient $X_j(t_0)$, enabling the determination of the deflection curve $y(x, t_0)$. With this information, the complete deflection time history $y(x, t)$ can be calculated. It is evident that installing more inclinometers leads to higher precision. Experimental findings indicate that a minimum of five inclinometers is required for a bridge span to achieve reliable results [18].

In a static test, the consideration of time is not necessary. By measuring the angular values of the inclination at n points on the bridge, a function of x can be determined to calculate the inclination throughout the structure.

Xingmin H. et al [18] conducted an experiment using a 6-meter-long beam. They installed six inclinometers equidistantly on the beam, with a micrometer placed between each neighboring inclinometer, as shown in Figure 3.4.

To simulate static loading, they used steel ingots. The results of this experiment are presented in Table 3.1. The estimated deflection values were accurate, with none of the values exceeding an error of 5%. A comparison between the inclinometer results (calculation) and the reads of micrometers (direct measurements) is shown in Figure 3.5.

## 3.2 Two inclinometers

In cases where five inclinometers are not available, the estimation of deflection can still be achieved using two or even just one inclinometer. Although this approach may yield a less precise approximation, it can still provide valuable insights into the deflection behaviour of the structure.

Figure 3.3: Fredericks Company's 0703-0711-99 ±3° Single-Axis Electrolytic Tilt Sensor [17]

Professor Francisco Queirós de Melo, from the Faculty of Engineering at the University of Porto, has developed a mathematical solution that can be applied in the deflection prediction of a simply supported beam. This program calculates a solution for four constants, $c_1$, $c_2$, $c_3$, and $c_4$, when given information about the structure's length, the position of the inclinometers and the values of inclination (in radians). These constants are determined by approximating the rotation to a fourth-degree function.

$$\frac{dy(x)}{dx} = \sum_{j=1}^{4} a_j g_j(x) \tag{3.3}$$

Where,

$$g_1(x) = 1$$
$$g_2(x) = x^2$$
$$g_3(x) = x^3$$
$$g_4(x) = x^4$$

Rewriting the Equation 3.3

$$\frac{dy(x)}{dx} = a_1 + a_2x^2 + a_3x^3 + a_4x^4 \tag{3.4}$$

Integrating this equation, we obtain

$$y(x) = a_1x + \frac{a_2}{3}x^3 + \frac{a_3}{4}x^4 + \frac{a_4}{5}x^5 \tag{3.5}$$

The constants that represent the solution of the problem are

$$c_1 = a_1$$
$$c_2 = \frac{a_2}{3}$$


Figure 3.4: Simple beam static experiment [18]

$$c_3 = \frac{a_3}{4}$$
$$c_4 = \frac{a_4}{5}$$

A graphical representation of deflection and rotation is presented in Figure 3.6 for a 1-meter beam. The inclinometer at x=0,25 $m$ indicates an inclination of $-2°$, while the inclinometer at x=0,75 $m$ indicates an inclination of $2°$.

## 3.3 Single inclinometer

### 3.3.1 Cantilever beam

When using only one inclinometer, it is necessary to calculate the shape functions for both the inclination and deflection. To illustrate this, a cantilever beam was considered, as shown in Figure 3.7, and used mechanics of materials to establish the relationship between load and deflection. This derivation is based on the Euler-Bernoulli beam theory, which neglects shear deformation. By considering the linear relationship between beam deflection and loads, which follows Hooke's Elasticity Law, we can determine the coefficients related to the stiffness properties of the material.

The deflection function $y(x)$ can be derived from the moment function.

$$\frac{d^2y(x)}{dx^2} = \frac{M(x)}{EI} \tag{3.6}$$

In the case of a cantilever beam, the moment can be expressed as

$$M(x) = Px - PL \tag{3.7}$$

By taking the first derivative of the Equation 3.7, we obtain the rotation function $\frac{dy(x)}{dx}$.

$$\frac{dy(x)}{dx} = \frac{1}{EI}\int px - PLdx = \frac{P}{EI}\left(\frac{x^2}{2} - Lx + C_1\right) \tag{3.8}$$

Taking the second derivative of Equation 3.7 (deriving the rotation function one time) gives us the deflection function $y(x)$.

Table 3.1: Results of Simple Beam Static Experiments [18]

| Angular value ($10^{-3}rad$) | Micrometer ($mm$) | Inclinometer ($mm$) | Relative error ($\%$) |
|---|---|---|---|
| 0,7068 | 0,449 | 0,429 | -4,39 |
| 0,6289 | 1,150 | 1,158 | 0,72 |
| 0,2518 | 1,420 | 1,445 | 1,73 |
| -0,2350 | 1,114 | 1,162 | 4,30 |
| -0,6140 | 0,438 | 0,427 | -2,42 |
| -0,6890 | | | |

$$y(x) = \frac{P}{EI}\int \frac{x^2}{2} - Lx + C_1 dx = \frac{P}{EI}\left(\frac{x^3}{6} - \frac{Lx^2}{2} + C_1 x + C_2\right) \tag{3.9}$$

To determine the constants $C_1$, and $C_2$, the geometric boundary conditions of the system need to be specified. These boundary conditions consist of two equations that provide the necessary information to solve for the two constants.

The displacement for x=0 is 0: $y_{(x=0)} = 0 \rightarrow C_2 = 0$

The rotation for x=0 is 0: $\frac{dy}{dx}_{(x=0)} = 0 \rightarrow C_1 = 0$

Resulting in the equations

$$\frac{dy(x)}{dx} = \frac{P}{EI}\left(\frac{x^2}{2} - Lx\right) \tag{3.10}$$

$$y(x) = \frac{P}{EI}\left(\frac{x^3}{6} - \frac{Lx^2}{2}\right) \tag{3.11}$$

A graphical representation of these two functions is shown in Figure 3.8, with unitary value for $\frac{P}{EI}$ and for L.

Having an inclinometer at x=c $(0 < c \leq 1)$, as represented in Figure 3.9, the value of $\frac{P}{EI}$ can be estimated with the equation

$$\tan(inc) = \frac{P}{EI}\left(\frac{c^2}{2} - cL\right) \tag{3.12}$$

Where inc represents the measured inclination value, using the inclinometer.

A test was conducted to obtain the rotation and deflection functions for the values c = 0,75, L=1 and inc = $-2°$, as shown in Figure 3.10.

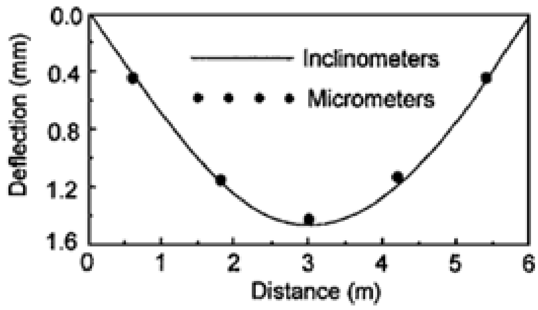


Figure 3.5: Comparison of inclinometer and micrometer results for a simple beam under static loads [18]

### 3.3.2 Simply supported beam

Considering now a simply supported beam, as illustrated in Figure 3.11, we can use the same method as before.

Considering that the load can be applied in any point of the beam, the behaviour of the left section differs from that of the right section. Therefore, it is necessary to divide the problem into two sections to account for these differences.

For section 1, $0 \leq x \leq a$,

$$M_1(x) = \frac{Pb}{L}x \tag{3.13}$$

$$\frac{d^2y}{dx^2} = \frac{M_1(x)}{EI}$$

$$\frac{dy_1}{dx} = \frac{P}{EI}\int \frac{b}{L}xdx = \frac{P}{EI}\left(\frac{b}{2L}x^2 + C_1\right) \tag{3.14}$$

$$y_1 = \frac{P}{EI}\int \frac{b}{2L}x^2 + C_1dx = \frac{P}{EI}\left(\frac{b}{6L}x^3 + C_1x + C_2\right) \tag{3.15}$$

For section 2, $a \leq x \leq 1$,

$$M_2(x) = \frac{Pb}{L}x - P(x-a) = P\left(a - \frac{ax}{L}\right) \tag{3.16}$$

$$\frac{d^2y}{dx^2} = \frac{M_1(x)}{EI}$$

$$\frac{dy_2}{dx} = \frac{P}{EI}\int a - \frac{ax}{L}dx = \frac{P}{EI}\left(-\frac{a}{2L}x^2 + ax + C_3\right) \tag{3.17}$$

$$y_2 = \frac{P}{EI}\int -\frac{a}{2L}x^2 + ax + C_3dx = \frac{P}{EI}\left(-\frac{a}{6L}x^3 + \frac{a}{2}x^2 + C_3x + C_4\right) \tag{3.18}$$

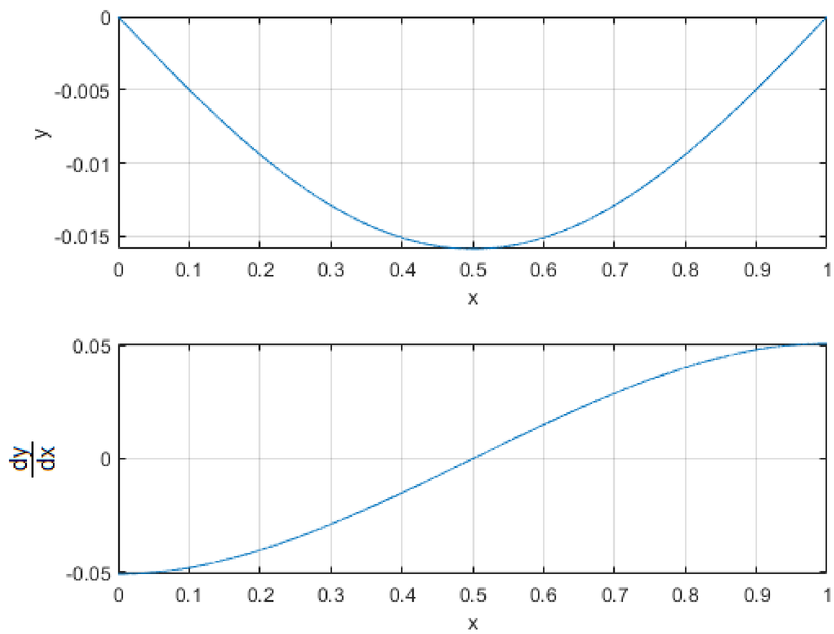


Figure 3.6: Graphical representation of the deflection y and the rotation $\frac{dy}{dx}$ of a simply supported beam with an inclination of $-2°$ at x=0,25 and $2°$ at x=0,75

Resulting in

$$y(x) = \begin{cases} \frac{P}{EI}\left(\frac{b}{6L}x^3 + C_1x + C_2\right); 0 \leq x \leq a \\ \frac{P}{EI}\left(-\frac{a}{6L}x^3 + \frac{a}{2}x^2 + C_3x + C_4\right); a < x \leq L \end{cases} \tag{3.19}$$

$$\frac{dy(\text{x})}{dx} = \begin{cases} \frac{P}{EI}\left(\frac{b}{2L}x^2 + C_1\right); 0 \leq x \leq a \\ \frac{P}{EI}\left(-\frac{a}{2L}x^2 + ax + C_3\right); a < x \leq L \end{cases} \tag{3.20}$$

To determine the values of $C_1$, $C_2$, $C_3$, and $C_4$, it is necessary to define the geometric boundary conditions and the continuity conditions of the system, which requires solving a set of four equations corresponding to these four constants.

The displacement for x=0 is 0: $y_{1(x=0)} = 0$

The displacement for x=L is 0: $y_{2(x=L)} = 0$

The displacement function needs to be continuous; this translates to: $y_{1(x=a)} = y_{2(x=a)}$

The rotation function needs to be continuous; this translates to: $\frac{dy_1}{dx}_{(x=a)} = \frac{dy_2}{dx}(x = a)$

The solution for the constants is obtained from these equations.

If we consider L=1, the variables x, a and b, can be defined as a fraction of the distance between zero and L, substituting L in the previous equations we obtain

$$C_1 = \frac{a\left(3La^2 - 2a^2 - 2a^2b - 6La + 3a^2 + 3ab + 3L - 1\right)}{-6L} \tag{3.21}$$

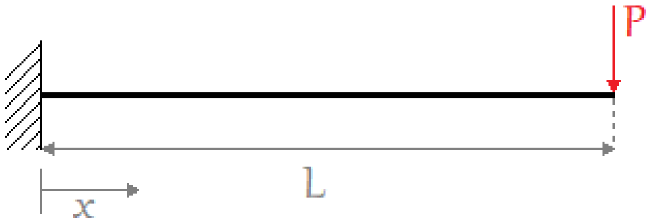


Figure 3.7: cantilever beam

$$C_2 = 0 \tag{3.22}$$

$$C_3 = \frac{a\left(3La^2 - 2a^3 - 2a^2b + 3L - 1\right)}{-6L} \tag{3.23}$$

$$C_4 = \frac{a^3(3L - 2a - 2b)}{6L} \tag{3.24}$$

A graphical representation of these two functions is shown in Figure 3.12, with unitary value for $\frac{P}{EI}$ and L, and a=0,5.

Having an inclinometer at x=c $(0 < \text{c} \leq 1)$, as represented in Figure 3.13, the value of $\frac{P}{EI}$ can be estimated with the equation

$$\tan(inc) = \left.\frac{dy(\text{x})}{dx}\right|_{x=c} \tag{3.25}$$

Where inc represents the measured inclination value, in degrees, using the inclinometer.

A test was conducted to obtain the rotation and deflection functions for the values of a=0,5, c = 0,25 and inc = $-2°$, as shown in Figure 3.14.

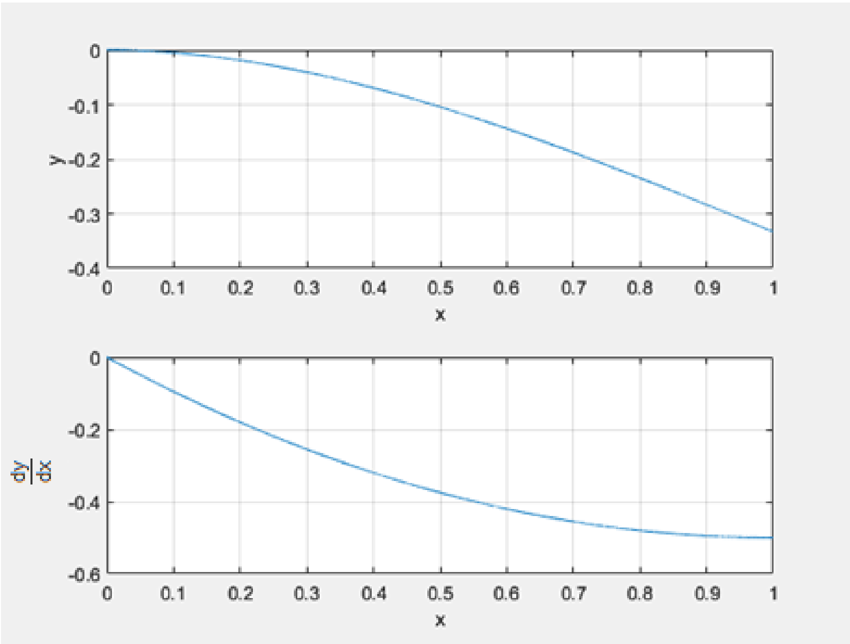


Figure 3.8: Graphical representation of the deflection y and the rotation $\frac{dy}{dx}$ of a cantilever beam

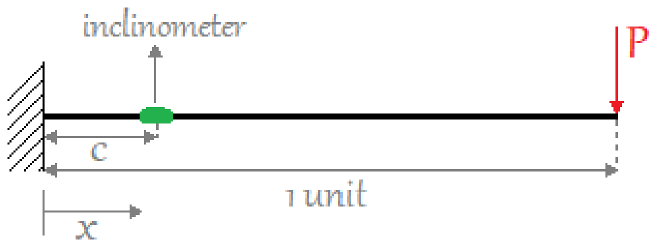


Figure 3.9: cantilever beam with an inclinometer at x=c

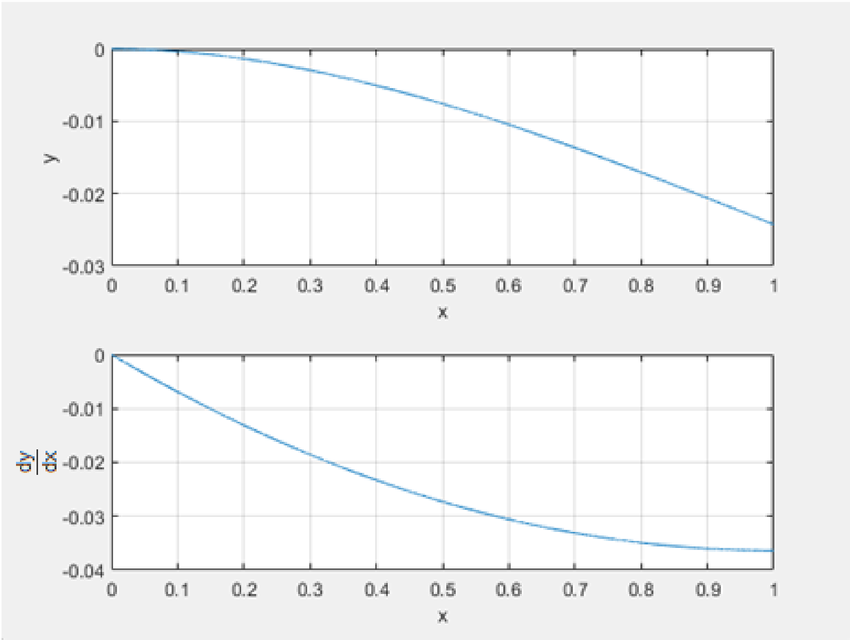


Figure 3.10: Graphical representation of the deflection y and the rotation $\frac{dy}{dx}$ of a cantilever beam with an inclination of $-2°$ at x=0,75

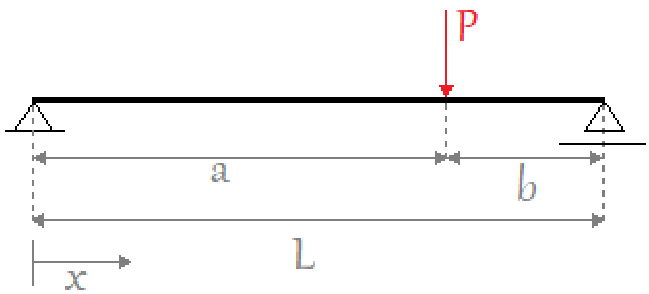


Figure 3.11: Simply supported beam loaded at x=a

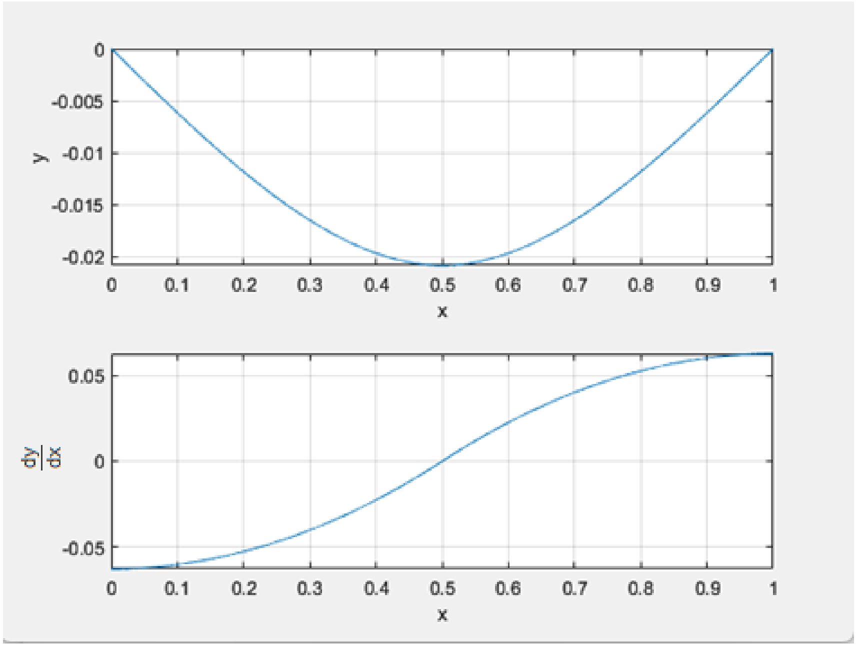


Figure 3.12: Graphical representation of the deflection y and the rotation $\frac{dy}{dx}$ of a simply supported beam with an applied load in the middle point, for a=0,5

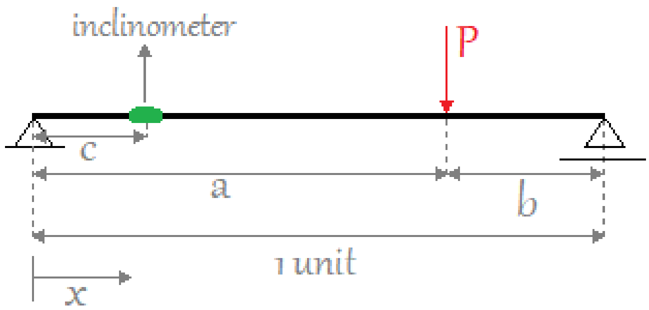


Figure 3.13: Simply supported beam with a load applied at x=a and an inclinometer at x=c

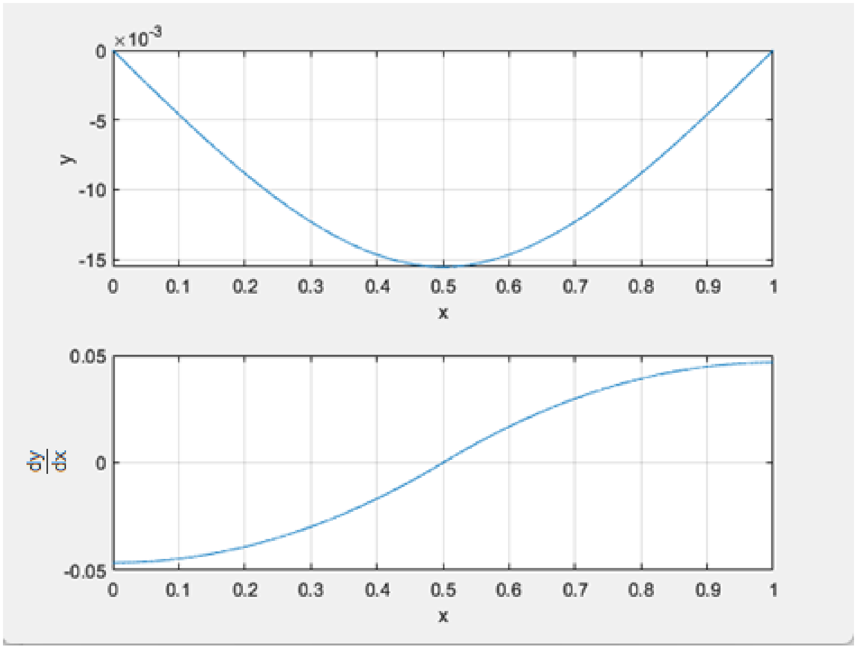


Figure 3.14: Graphical representation of the deflection y and the rotation $\frac{dy}{dx}$ of a simply supported beam with an applied load in the middle point, for a=0,5 and an inclination of $-2°$ at x=0,25

# Chapter 4

# Inclinometers Methods Testing

Replicating the behaviour of a bridge in a laboratory setting is a challenging task that involves considering various factors such as structural properties, material behaviour, loading conditions, and boundary conditions. It is important to acknowledge that laboratory replication is a simplified representation and may not fully capture all the complexities of real-world bridge behaviour.

To validate the accuracy and reliability of the inclinometer methods for deflection calculation, a laboratory test was conducted. The test aimed to replicate a bridge scenario with a concentrated load.

A simply supported beam with a concentrated load at x=a was chosen for this replication, as depicted in Figure 3.11. In the laboratory case, the external concentrated load had a more significant impact on the beam's deflection compared to its self-weight. Therefore, for simplicity, the weight of the beam was not considered in the calculations. It is important to note that in a real bridge, the weight of the structure would have a more significant influence on its deformation, and this approximation would not be applicable.

## 4.1 Preparation

In place of the bridge, a steel beam with a rectangular cross-section was employed as a substitute. This beam had an effective length of 1,2 meters, a width of 50 millimetres and a thickness of 3 millimetres.

The supports needed to allow rotation and movement in the horizontal direction. To meet these requirements, it was decided to use a stool and a cylinder for each support. There were two equal stools and the cylinders used had the same diameter.

To ensure proper alignment and positioning of the supports, the stools were marked with a pencil, Figure 4.1. The cylinders were then adjusted to align with the marked positions on the stools and securely fixed in place using tape, Figure 4.2.

Figure 4.1: Stool marked with pencil

Once the cylinders were securely attached, the stools were positioned with a spacing of 1,2 meters between supports. To ensure their positioning, a mark was made on the ground as a visible reference in case the stools shifted or moved. This mark served as a guide to easily realign and reposition the stools, if necessary, Figure 4.3.

After preparing the supports, marks were made on both the floor and the beam. These marks were essential for positioning the load and facilitating the measurement of deflection and inclination, Figure 4.4.

As a last step, it was made sure that the beam was aligned with the supports, Figure 4.5.

## 4.2 Instrumentation

A magnetic inclinometer,AUTOUTLET Digital Level Box [31], depicted in Figure 4.6, was utilized to measure the inclination. This inclinometer provides an accuracy of ±0,1 degrees and a resolution of 0,05 degrees. It was set at x=0, as this is the point where the maximum inclination occurs.

To measure the deflection at various points of the beam, a RS PRO RSLDM-35H laser distance meter [32], shown in Figure 4.7, was employed. This distance meter offers an accuracy of ±1,5 millimetres and a resolution of 1 millimetre.

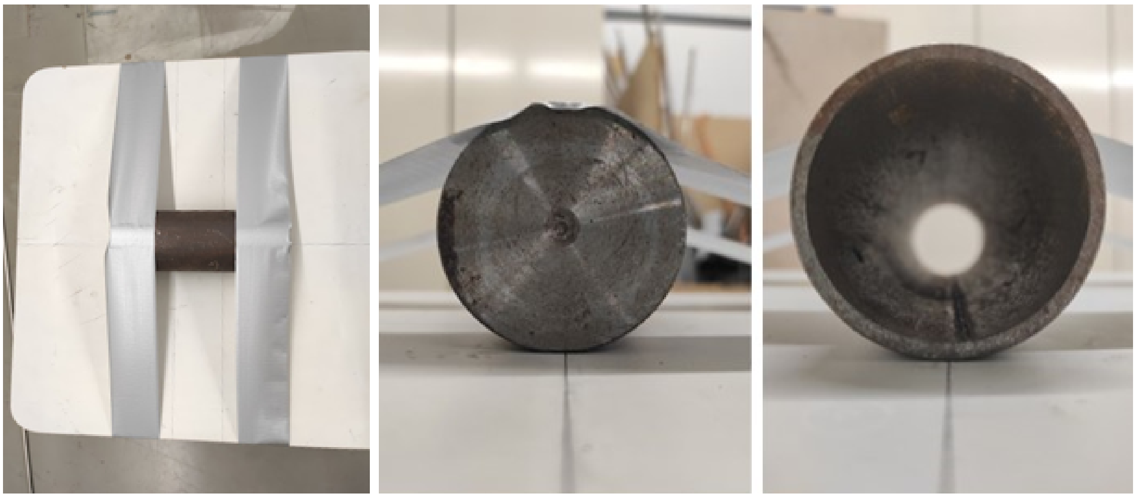

Figure 4.2: Cylinders aligned and fixed to the stool

## 4.3 Testing

Before starting the testing, it was necessary to verify that the inclination with respect to both supports was zero. To do this, a rigid cylindrical bar was used, and its inclination was measured. The height of the stools was adjusted until the initial inclination reading was determined to be zero, measuring shown in Figure 4.8.

Once the beam was positioned and adequately instrumented, it was ready to be subjected to a load. Two tests were conducted, both involved placing weights at the centre of the beam, the difference between them was the weight used.

To prevent the large surface area of the weights from directly contacting the beam, a small cylinder was utilized as a point of contact between the beam and the weights. This ensured a more localized load distribution on the beam. The arrangement of the weights and the location of the inclinometer can be observed in Figure 4.9.

## 4.4 Results and analysis

### 4.4.1 Single inclinometer

Once all the measurements were completed, the deflection was calculated based on the inclination, and the results are presented in Table 4.1.

Upon comparing the measured deflection with the calculated deflection, it is observed that the error for the maximum deflection is small, not exceeding 2,5%. A comparison between the measured and calculated deflection is shown in Figure 4.10

The same experiment was repeated using a regular smartphone with an installed app (called "Nível Perfeito") to measure the inclination, and the results are presented in Table 4.2.

Table 4.1: Results for simply supported beam

| Test | Inclination ($degrees$) | Measured deflection ($mm$) | Calculated deflection ($mm$) | Relative error ($\%$) |
|---|---|---|---|---|
| 1 | -4,50 | 18 | 18,0 | 0,00 |
| | | 26 | 26,2 | 0,77 |
| | | 18 | 18,0 | 0,00 |
| 2 | -6,85 | 30 | 27,5 | -8,33 |
| | | 41 | 40,0 | -2,44 |
| | | 29 | 27,5 | -5,17 |

Table 4.2: Results for simply supported beam (inclination measured with a smartphone)

| Test | Inclination ($degrees$) | Measured deflection ($mm$) | Calculated deflection ($mm$) | Relative error ($\%$) |
|---|---|---|---|---|
| 1 | -4,60 | 18 | 18,4 | 2,22 |
| | | 26 | 26,8 | 3,08 |
| | | 18 | 18,4 | 2,22 |
| 2 | -6,70 | 30 | 26,9 | -10,33 |
| | | 41 | 39,2 | -4,39 |
| | | 29 | 26,9 | -7,24 |

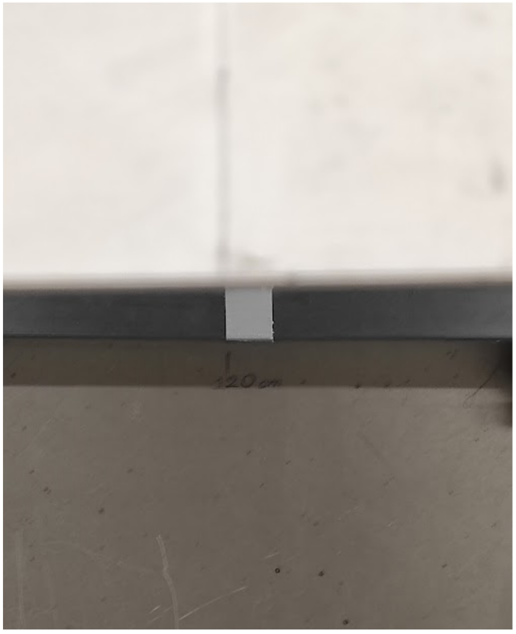

Figure 4.3: Alignment of the stools with the floor

A comparison between the measured and the calculated deflection was conducted, and depicted in the Figure 4.11.

Comparing the error between the inclinometer and the smartphone, it can be concluded that the error has increased; however, it is still acceptable as the error for the maximum deflection does not exceed 5%. A comparison between the measured and calculated deflection for the smartphone is shown in Figure 4.11.

### 4.4.2 Two inclinometers

To validate the effectiveness of the two inclinometers method, a test equivalent to test 2 was conducted, with the inclinometer positioned at x=0 *m* and the smartphone at x=1,2 *m*. The results for this test are presented in Table 4.3, and a comparison between the measured and predicted deflection is shown in Figure 4.12.

It is observed that the beam's inclination is not symmetrical, despite the weights being applied in the middle of the beam. This unexpected asymmetry may be attributed to pre-deformation of the beam.

This method yields a higher relative error in the maximum deflection compared to the previous approach. However, the error across the entire beam is smaller. Additionally, it should be noted that this approach tends to provide conservative estimates, resulting in larger deflection values than the actual ones. Further testing is recommended to determine if this characteristic is consistent or occurred by chance.

Figure 4.4: Floor and beam marks

## 4.5 Real-life applications

In real bridges, the self-weight of the structure cannot be disregarded. Therefore, if using the single inclinometer method, it is necessary to include a distributed load that corresponds to this component. Real-life structures are composed of different materials, resulting in varying Young's modulus and moment of inertia. Consequently, it is not possible to predict deflection with absolute zero error, nor is it the objective. The aim is to predict deflection with a relatively low error that allows for the observation and detection of critical behaviour, enabling timely actions to prevent catastrophes.

The choice of inclinometers depends on the characteristics of the structure, such as its susceptibility to deformation and the impact of slight changes in inclination on the analysis. Establishing the plane of zero inclination is crucial for these methods. This reference plane may not align with the absolute zero in relation to gravitational acceleration, as it depends on the inclination between supports.

As demonstrated, monitoring a structure does not necessarily require a complex system. For simple structures, it is more cost-effective and efficient to implement a simple monitoring system. In the case of inclination measurement, even a regular smartphone can be utilized since most smartphones now come equipped with an accelerometer sensor.

In more autonomous systems, the data from inclinometers can be processed and translated into deflection values. In critical cases, an external actuator can be employed to provide visible and noticeable signs of danger, such as gates, traffic lights, or variable message signs. These indicators help keep the public informed and updated about the safety of the structure.

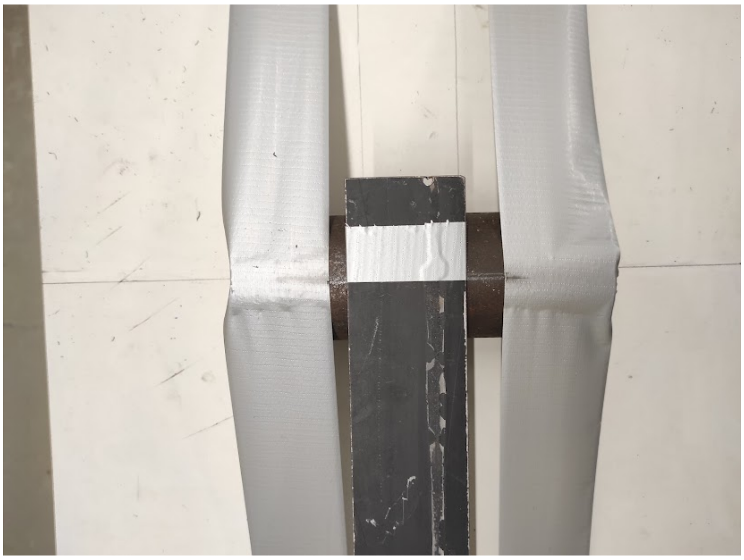

Figure 4.5: Alignment of the beam with the support


Figure 4.6: Inclinometer used


Figure 4.7: Laser distance meter used

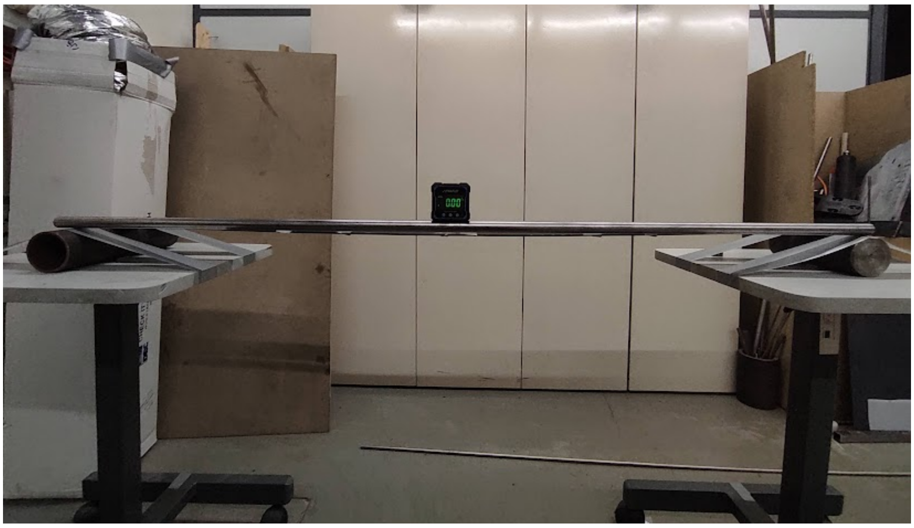

Figure 4.8: Measuring inclination with respect to both supports

a) b)

Figure 4.9: a) setup for test 1, b) setup for test 2

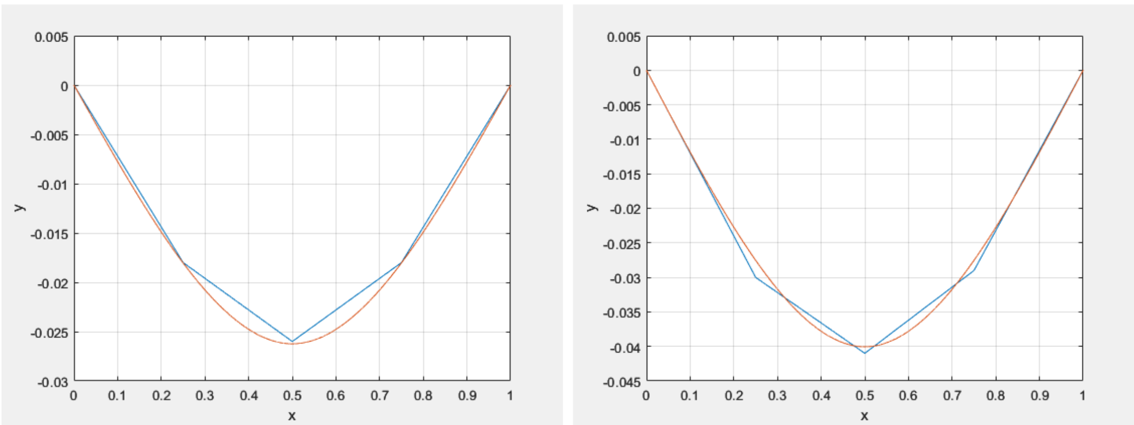


a) b)

Figure 4.10: Comparisson between the measured (blue) and the calculated (orange) deflection; a) test 1, b) test 2

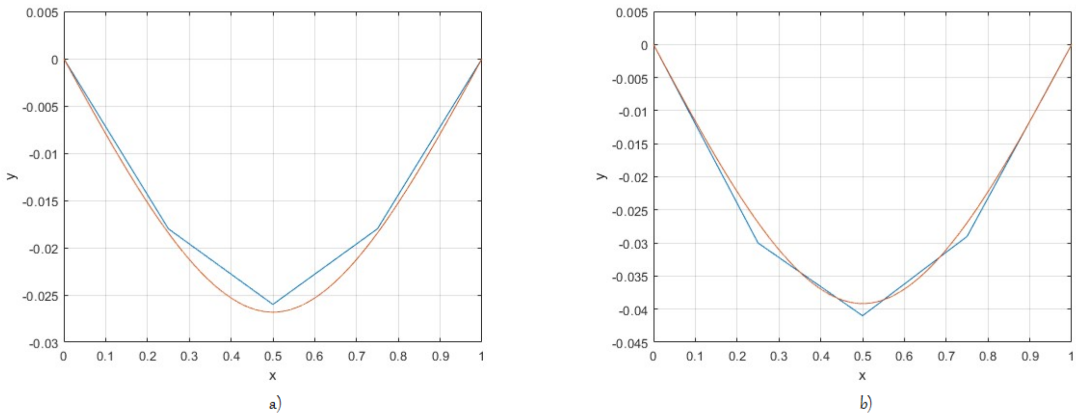


Figure 4.11: Comparisson between the measured (blue) and the calculated (orange) deflection using a smartphone; a) test 1, b) test 2

Table 4.3: Results for simply supported beam, inclination 1 measured with the inclinometer, inclination 2 measured with a smartphone

| Inclination 1 *(degrees)* | Inclination 2 *(degrees)* | Measured deflection *(mm)* | Calculated deflection *(mm)* | Relative error *(%)* |
|---|---|---|---|---|
| | | 30 | 31,6 | 5,33 |
| -6,80 | 6,6 | 41 | 43,9 | 7,07 |
| | | 29 | 30,9 | 6,55 |

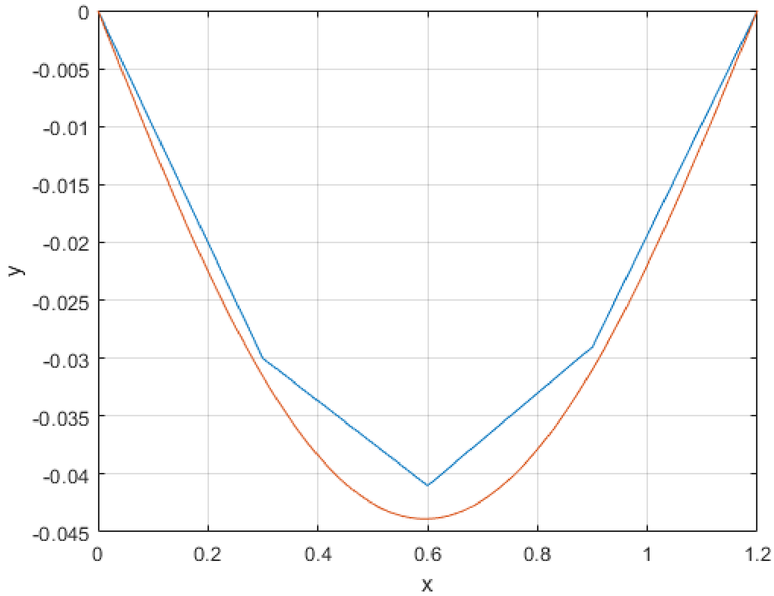


Figure 4.12: Comparisson between the measured (blue) and the calculated (orange) deflection using a inclinometer and a smartphone

# Chapter 5

# Conclusion

Ensuring the safety and integrity of infrastructure is a paramount concern in the field of engineering. Deflection, as a significant indicator of a structure's safety condition, poses challenges when it comes to direct measurement. The primary objective of this dissertation was to investigate a simple and practical approach for monitoring structural health by utilizing inclinometers to predict deflection. Inadequate inspection and monitoring of existing structures contribute to the unsatisfactory condition of bridge infrastructure. Effective monitoring plays a crucial role in preventing catastrophic bridge failures, exemplified by tragic incidents such as the collapse of the "Entre-os-Rios" bridge in Portugal and the Morandi bridge in Italy, which resulted in numerous casualties. However, one of the main challenges in structural health monitoring is the cost associated with implementing monitoring systems. By utilizing low-cost sensors like inclinometers, monitoring becomes more accessible and feasible. Inclinometers come in various types based on their operational principles. Mechanical inclinometers, the simplest type, do not require a power source or calibration, while more sophisticated inclinometers offer increased precision and resolution. Multiple approaches can be employed to predict deflection based on inclinometer measurements. A method proposed by Xingmin Hou et al. [18], by utilizing more than five inclinometers, demonstrates promise in accurately measuring bridge deflection in both static and dynamic scenarios. Alternatively, a more simplified approach can be achieved with just two or even a single inclinometer. Experimental tests were conducted using the latter two methods, and the results demonstrated a satisfactory approximation of deflection. Notably, even a common device like a smartphone can be used for inspection purposes when inclinometers are unavailable, and it still provides a good estimation of deflection. Further experimentation would be beneficial, particularly by studying real bridge structures. Additionally, integrating any of these methods into a system capable of closing a bridge in case of safety concerns would be an interesting prospect. In summary, the findings of this study present cost-effective solutions for structural monitoring. The proposed inclinometer-based methods exhibit significant potential for implementation in bridges worldwide, contributing to enhanced safety and structural integrity.

# Appendix A

## A.1 MATLAB scripts

```
%script to calculate the deflection and rotation
%fixed beam under load at the free edge
l= input('enter l: ');
c= input('enter c: '); %position of the inclinometer (0<c<=1)
inc=input('enter degrees: '); %value of inclination in degrees
x=0:0.0001:1;
y=((x.^3)/6-(x.^2)/2);
dy=((x.^2)/2-x);
nn=((length(x)-1)/(1/c))+1;
ci=tan(inc*pi/180)/dy(nn); %ci is the aproxiamation for P/EI
y2=y*ci*l;  % y2 is the defletion with the correction of the value of inclination
dy2=dy*ci; % dy2 is the rotation with the correction of the value of inclination

figure(1)
subplot(2,1,1)
plot(x,y2)
xlabel('x')
ylabel('y')
grid on
subplot(2,1,2)
plot(x,dy2)
xlabel('x')
ylabel('dy')
grid on
```

Figure A.1: MATLAB script to calculate the deflection and rotation of a fixed beam under load at the free edge, knowing only one value of the inclination, in degrees, at x=c

```
%simply suported beam, load at any point
l= input('enter l: ');
a= (input('enter a: '));
c= (input('enter c: ')); %position of the inclinometer (0<c<=1)
inc=input('enter degrees: ');%value of inclination in degrees
x=0:0.0001:1;
b= 1-a;
c1=(1/3)*a^4+(1/3)*b*a^3-a^3-(1/2)*a^2*b+a^2-(1/3)*a;
c2=0;
c3=-(1/3)*a+(1/3)*a^4+(1/3)*b*a^3-(1/2)*a^3;
c4=-(1/3)*a^4-(1/3)*b*a^3+(1/2)*a^3;
n=a*10000+1;
v=zeros(1,length(x));
dv=zeros(1,length(x));
for j=1:n
    v(j)=(1/6)*b*x(j).^3+c1*x(j)+c2;  %deflection for section 1
    dv(j)=(1/2)*b*x(j).^2+c1;      %rotation for section 1
end
for j=n+1:length(x)
    v(j)=-(1/6)*x(j).^3*a+(1/2)*a*x(j).^2+c3*x(j)+c4;  %deflection for section 2
    dv(j)=-(1/2)*a*x(j).^2+a*x(j)+c3;             %rotation for section 2
end
nn=c*10000+1;
ci=tan(inc*pi/180)/dv(nn); %ci is the aproxiamation for P/EI

v2=v*ci*l; % v2 is the defletion with the correction of the value of inclination
dv2=dv*ci; % dv2 is the rotation with the correction of the value of inclination

figure(1)
subplot(2,1,1)
plot(x,v2)
xlabel('x')
ylabel('y')
grid on
subplot(2,1,2)
plot(x,dv2)
xlabel('x')
ylabel('dy')
grid on
```

Figure A.2: MATLAB script to calculate the deflection and rotation of a simply supported beam loaded at x=a, knowing the inclination, in degrees, at x=c

# Appendix B

## B.1 Two inclinometer program

```
 Matrix size N refers to a 5th order polynomial
 reduced to 4 factors to determine
 Bridge length between supports (base10 exponent!) RL=
1.2
 Indicate the non-dimensional coordinate of inclinometer
 position; for example fraction of the bridge length
 as posin1=0.25 and posin2=0.75

 position of posin1(decimal)=
0
 position of posin2(decimal)=
1
 Matriz factor reading; attention: by columns!
 Identification by direct exression
 AINV(            1 ,            1 )=  6.0533182386816710８E-016
 AINV(            1 ,            2 )=  8.2190555801604863５E-017
 AINV(            1 ,            3 )=  0.99999999999999967
 AINV(            1 ,            4 )= -3.62028155974615930E-016
 AINV(            2 ,            1 )=   5.7870370370370408
 AINV(            2 ,            2 )=  0.41666666666666702
 AINV(            2 ,            3 )=  -4.1666666666666679
 AINV(            2 ,            4 )=  -2.7777777777777799
 AINV(            3 ,            1 )=  -7.2337962962962994
 AINV(            3 ,            2 )= -0.69444444444444486
 AINV(            3 ,            3 )=   4.6296296296296306
 AINV(            3 ,            4 )=   4.0509259259259283
 AINV(            4 ,            1 )=   2.4112654320987663
 AINV(            4 ,            2 )=  0.28935185185185197
 AINV(            4 ,            3 )=  -1.4467592592592593
 AINV(            4 ,            4 )=  -1.4467592592592600
 Now include RHS values (Inclinometer angles)
 Angle at left side position=
-0.1187
 Angle at right side position=
0.1152
 resul(           1 )= -0.11870000000000000
 resul(           2 )=  0.17458333333333326
 resul(           3 )= -8.28703703703702332E-002
 resul(           4 )=  5.06365740740732668E-003
 Define the final polynomial shape function
 How many points for graphic plot? Nponts=
```

Figure B.1: Executable program used to calculate the deflection with two values of inclination

# Referências


[1] M. Holroyd, “Victims of Portugal’s deadly bridge collapse remembered 20 years on.” https://www.euronews.com/2021/03/04/victims-of-portugal-s-deadly-bridge-collapse-remembered-20-years-on, mar 4 2021.

[2] B. S. Bettiza, “Genoa bridge disaster: Risk of collapse ’was known for years’.” https://www.bbc.com/news/world-europe-65684334, may 23 2023.

[3] G. S. Reporter, “What caused the Genoa bridge collapse – and the end of an Italian national myth?.” https://www.theguardian.com/cities/2019/feb/26/what-caused-the-genoa-morandi-bridge-collapse-and-the-end-of-an-italian-national-myth, sep 23 2020.

[4] L. Bisby and M. Briglio, “Isis and samco educational module 5 : An introduction to structural health monitoring,” 2005.

[5] level developments, “5789/1 - Bubble Inclinometer.” https://www.leveldevelopments.com/products/inclinometers/ball-bubble-inclinometers/57891-bubble-inclinometer-100x25mm-3/, apr 20 2023.

[6] C. . Plath, “Pendulum Clinometer triangular.” https://shop.cassens-plath.de/en/nautical-inventory/clinometer/243/pendulum-clinometer-triangular.

[7] R. inc., “2110-D Mechanical Inclinometer - Rieker Inc..” https://www.riekerinc.com/shop/mechanical-inclinometers/2110-d-inclinometer/, jun 12 2023.

[8] J. Dunnicliff, *GEOTECHNICAL INSTRUMENTATION FOR MONITORING FIELD PERFORMANCE*. Wiley-Interscience, 1993.

[9] E. N. Hernandez, “Us4088027a - Force balance servo accelerometer - Google Patents.” https://patents.google.com/patent/US4088027A/en, sep 29 1976.

[10] D. Ha, H. Park, S. W. Choi, and Y. Kim, “A wireless mems-based inclinometer sensor node for structural health monitoring,” *Sensors (Basel, Switzerland)*, vol. 13, pp. 16090–104, 12 2013.

[11] S. Trivedi, T. Shen, C.-Y. Chang, P.-W. Huang, and S.-S. Li, “Design of piezoelectric mems accelerometer module and its application in surface roughness prediction of fused silica substrate,” *IEEE Sensors Journal*, vol. 21, no. 19, pp. 21979–21988, 2021.

[12] R. Mukhiya, P. Agarwal, S. Badjatya, M. Garg, P. Gaikwad, S. Sinha, A. K. Singh, and R. Gopal, “Design, modelling and system level simulations of drie-based mems differential capacitive accelerometer,” *Microsystem Technologies*, vol. 25, pp. 3521–3532, Sep 2019.

[13] R. Mukherjee, J. Basu, P. Mandal, and P. K. Guha, "A review of micromachined thermal accelerometers," *Journal of Micromechanics and Microengineering*, vol. 27, p. 123002, nov 2017.

[14] M. Ahmadian, K. Jafari, and M. J. Sharifi, "Novel graphene-based optical mems accelerometer dependent on intensity modulation," *ETRI Journal*, vol. 40, no. 6, pp. 794–801, 2018.

[15] Amazon, "Gate14® Inclinómetro náutico de dupla bolha de precisão : Amazon.es: Bricolage e Ferramentas." https://www.amazon.es/-/pt/dp/B08YZ5S5LZ/ref=sr_1_5?crid=10U8XNEW2QTAGkeywords=mechanical+ inclinometerqid=1686755222sprefix=mechanical+inclinometer%2Caps%2C149sr=8-5.

[16] Neoteck, "Neoteck Backlight LCD Digital Angle Finder - Red." https://neoteck.cn/products/neoteck-backlight-lcd-digital-angle-finder-red.

[17] F. Company, "0703-0711-99 ±3° Single-Axis Electrolytic Tilt Sensor - Fredericks." https://www.frederickscompany.com/products/0703-0711-99/, may 12 2023.

[18] X. Hou, X. Yang, and Q. Huang, "Using inclinometers to measure bridge deflection," *Journal of Bridge Engineering*, vol. 10, no. 5, pp. 564–569, 2005.

[19] I. de Portugal, "Nova edição dos 50 desafios de inovação da ip." https://www.infraestruturasdeportugal.pt/pt-pt/nova-edicao-dos-50-desafios-de-inovacao-da-ip.

[20] Y. Dong, R. Song, and H. Liu, "Bridges structural health monitoring and deterioration detection - synthesis of knowledge and technology," Dec 2010. Tech Report.

[21] Baumer, "Function of Strain Sensors | Baumer Switzerland." https://www.baumer.com/ch/en/service-support/function-principle/function-of-strain-sensors/a/function-strain-sensors.

[22] E. Rite, "Inclinometer: Types, how it works." https://www.encardio.com/blog/inclinometer-types-how-it-works-uses, may 9 2023.

[23] A. S. Algamili, M. H. M. Khir, J. O. Dennis, A. Y. Ahmed, S. S. Alabsi, S. S. Ba Hashwan, and M. M. Junaid, "A review of actuation and sensing mechanisms in mems-based sensor devices," *Nanoscale Research Letters*, vol. 16, p. 16, Jan 2021.

[24] Y. Q. Ni, X. W. Ye, and J. M. Ko, "Monitoring-based fatigue reliability assessment of steel bridges: Analytical model and application," *Journal of Structural Engineering*, vol. 136, no. 12, pp. 1563–1573, 2010.

[25] Posital, "Mems Inclinometer from POSITAL: How do they work?." https://www.posital.com/en/products/inclinometers/mems/MEMS-Technology.php:~:text=Inclinometersnov 28 2012.

[26] Renkeer, "Inclinometer & tilt sensor working, types and applications." https://www.renkeer.com/inclinometer-working-types-and-applications/.

[27] O. Engineering, "Wheatstone bridge for strain gauges." https://www.omega.com/en-us/resources/wheatstone-bridge, may 27 2023.

[28] L. C. F. Coimbra, “Uma perspetiva operacional sobre a aplicação de inclinómetros no âmbito da geotecnia,” 2019.

[29] M. Tilli, M. Paulasto-Krockel, V. M. Airaksinen, S. Franssila, V. Lindroos, A. Lehto, and T. Motooka, *Handbook of Silicon Based MEMS Materials and Technologies*. Elsevier, dec 8 2009.

[30] R. Lan, Y. Wang, and Q. Chi, “Reconstitution of static deflections of suspension bridge based on inclinometer data,” *IOP Conference Series: Earth and Environmental Science*, vol. 304, p. 032081, sep 2019.

[31] AUTOUTLET. https://autoutlet.cn/collections/inclinometer/products/autoutlet-digital-level-box-protractor-angle-finder-level-gauge-waterproof.

[32] R. PRO. https://uk.rs-online.com/web/p/laser-measures/1268820.